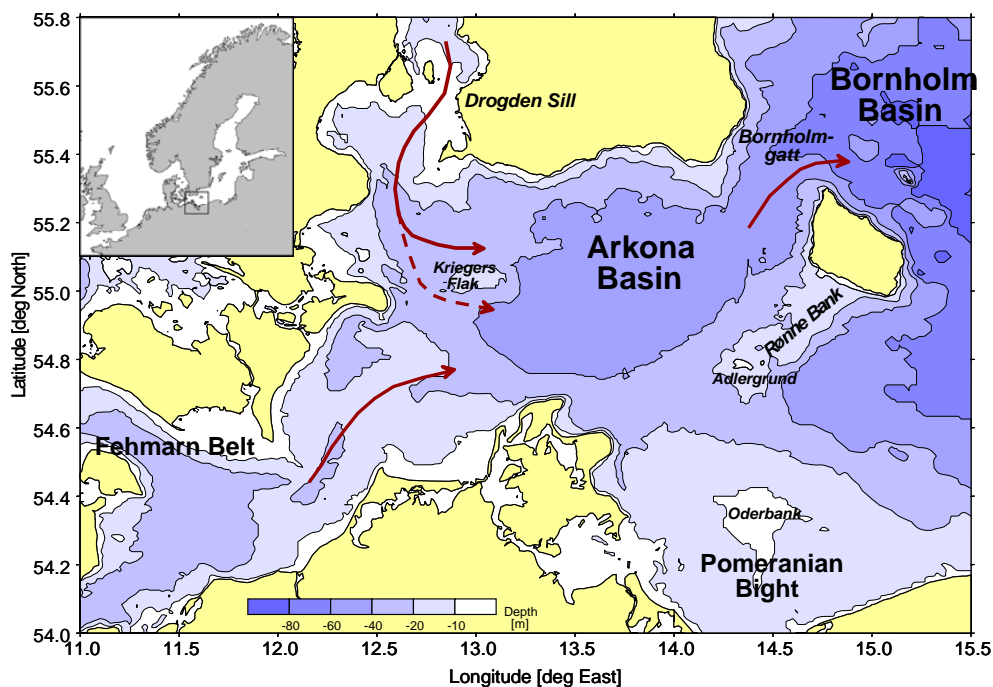


**Report**



**Possible hydrographical effects upon inflowing deep water of a pipeline crossing the flow route in the Baltic Proper**

**Karin Borenäs, Anders Stigebrandt**

*Cover picture.*

*The picture shows the bathymetry of the Arkona Basin and parts of the Bornholm Basin (courtesy of: Leibniz Institute for Baltic Sea Research, Warnemünde Germany)*

# Possible hydrographical effects upon inflowing deep water of a pipeline crossing the flow route in the Bornholm Proper

**Karin Borenäs, Anders Stigebrandt**

Author SMHI SE 601 76 Norrköping Sweden	Project Leader Kjell Wickström +46 11 495 83 11 kjell.wickstrom@smhi.se
Client Ramboll Oil & Gas Teknikerbyen 31 2830 Virum Denmark	Contact Henning Smith Nielsen +45 4598 6000 hsn@ramboll.dk
Distribution Ramboll	
Classification Confidential	
Keywords oceanography, salinity, oxygen, deep water inflow, gas pipeline	
Other	



## Contents

1	SUMMARY.....	1
2	BACKGROUND.....	2
3	HYDROGRAPHY OF THE BALTIC PROPER.....	3
4	CURRENTS IN THE WESTERN PART OF THE BALTIC SEA ...	7
4.1	General description.....	7
4.2	Observed bottom currents .....	7
4.3	Modeled currents.....	12
4.4	Density stratification close to the bottom.....	15
5	THE GOTLAND SEA .....	15
6	PROPERTIES OF WATER EXCHANGE.....	18
7	DYNAMICS OF THE DEEPWATER FLOW.....	19
7.1	Frictional flow and mixing .....	19
7.2	Hydraulic flow and upstream influence.....	20
7.3	Topographic steering.....	21
8	INTERACTION BETWEEN THE FLOW OF NEW DEEPWATER AND THE PIPELINES.....	22
8.1	Frictional flow .....	22
8.2	Hydraulic flow .....	23
8.3	Topographic steering.....	23
9	CREATION AND EFFECTS OF PIPELINE DAMS.....	24
10	EFFECTS ON STRATIFICATION AND OXYGEN CONDITIONS IN THE BALTIC PROPER .....	24
11	CONCLUSIONS.....	26
12	REFERENCES.....	27
13	APPENDICES .....	30



# 1 Summary

The new deepwater flowing through the Arkona and Bornholm Basins supplies oxygen and salt to the deepwater of the Baltic Proper. It is therefore vital for the physical, biogeochemical and ecological states of the Baltic Proper. The properties of the new deepwater are subjected to quite large changes in these basins due to entrainment of residing less saline and oxygen rich water. In this report we estimate the impact of the planned Nord Stream pipelines on the salinity, volume flow and oxygen concentration of new deepwater in the Baltic Proper.

At present the turbulence created by the dense bottom current is due to bottom and interfacial mixing. The total dissipation of the dense bottom current, i.e. the dissipation integrated from the entrance sills in Fehmarn Belt and Öresund to Stolpe Channel, is essentially determined by the potential energy of the dense water when passing the sills. The mixing of the new deepwater might increase if the mixing efficiency of pipeline-generated turbulence,  $R_{f_{pipe}}$ , is greater than that of turbulence generated by the present combination of bottom and interfacial friction,  $R_f$  ( $R_f=0.04$ ).

It is found that if the Nord Stream pipelines rise 1.0 m above the sea bed they are capable to dissipate up to 0.5 % of the total potential energy, depending on the speed of the dense bottom current in the crossing section. If the mixing efficiencies are equal, i.e.  $R_{f_{pipe}}=R_f$ , there should in essence be no impact of the pipelines on the properties of new deepwater. Using  $R_{f_{pipe}}=0.12$ , which is conservative, it is estimated that the increased mixing of the new deepwater will be in the interval 0-1.0 %. In the Gotland Basin a possible increase in mixing due to the pipelines should be less than in the Bornholm Basin owing to generally lower velocities.

During large inflow events the Bornholm Strait and the Stolpe Channel may hydraulically control the transports from the Arkona and Bornholm Basins, respectively, into the Baltic Proper. Since the pipelines will not pass through these constrictions there will be no hydraulic effect on the flow. The same holds for the route in the East and North Gotland Sea where the pipelines will not cross any sill crests.

A possible topographic steering of the inflow, as it passes the pipelines on a sloping bottom, will be of minor importance and it is estimated that less than 1.7% of the inflow can be diverted down the slope by this mechanism in the Bornholm Basin. Since the mixing properties of a diverted flow will be the same as for the main inflow, any effect of topographic steering will be negligible. In the Gotland Basin topographic steering is not relevant.

Increased mixing of new deepwater by 0-1.0% means that deepwater salinity decreases by 0- 0.02 psu and that both the flow rate and the oxygen transport increase by 0- 1.0%. Such changes are very small compared to the natural variations why they cannot have any effect on density driven transport of new deepwater into the northern parts of the Baltic proper. Increased volume flow will not change the volume of deepwater of the Baltic proper but it decreases its residence time. Therefore, increased transport of oxygen would tend to improve the oxygen conditions in, and below, the halocline in the Baltic Proper and thereby increase the

deposition of phosphorus in the deepwater. Although the effect is very small, the pipelines may thus tend to decrease the effects of eutrophication of the Baltic Proper.

The estimated total area of dams (caused by closed depth contours) created by the pipeline in the depth interval 40-80 m is less than 25 km<sup>2</sup> why they cover less than 0.06% of the bottom area in that depth interval. Temporary accumulation of denser water and possibly following anoxia in the dams will therefore have negligible influence on the phosphorus sinks in the Baltic proper.

## **2 Background**

Nord Stream is composed of two parallel gas pipelines that will run through the Baltic Sea from Vyborg, Russia to Greifswald, Germany. The proposed route for the pipelines goes south of Bornholm, see *Figure 1*.

The inner diameter is fixed to 1153 mm throughout the entire pipe. The outer diameter can vary due to varying wall thickness (different pressure classes), small variation in outer coating and different requirements for outer concrete ballast (depends on bottom stability). However as a conservative assumption the outer diameter is in this context set to 1.5 m which is not exceeded at any sections of the pipelines. However, the pipes will sink into the bottom sediments why the mean height above the bottom will be 1.0 meter.

The objective of this report is to describe the general oceanographic conditions in the western part of the Baltic Sea and to discuss and estimate possible effects that the planned pipelines may have upon the flow of new deepwater into the Baltic Proper and its downstream properties. The pipelines may also create shallow dams, defined by closed depth contours. The dams may accumulate denser water that possibly may develop anoxia. The possible effect of this upon the phosphorus sink in the Baltic proper will also be discussed.



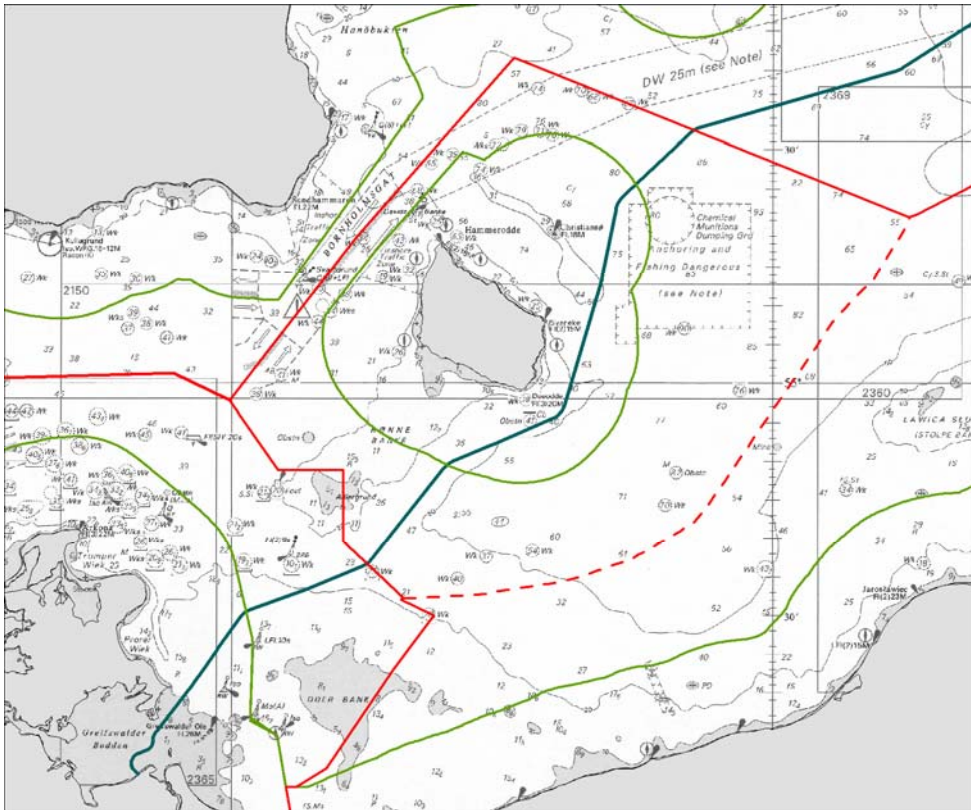


Figure 1. Projected route (solid blue line) of Nord Stream.

### 3 Hydrography of the Baltic Proper

The Baltic proper is characterized by an extensive freshwater excess that produces a strong stratification. In the upper layer the salinity is rather constant whereas large variations are found in the deeper parts. These are due to the sporadic inflows of more saline water. The temperature is subjected to seasonal changes and deviations from the mean temperature may be large. The vertical density distribution is mainly determined by the salinity and in the south-western Baltic Sea the largest variations are found in the deeper parts of the water column. Vertical profiles of the observed temperature, salinity, density and oxygen have been compiled for 4 hydrographic stations (BY2, BY5, BY15 and BY20) in the Baltic Proper (for the positions, see *Figure 2*). Climatological averages and standard deviations at standard depths are presented in Appendix A.



Figure 2. Position of hydrographic stations at which vertical profiles of temperature, salinity and oxygen are measured on a regular basis. Stations marked with red pertain to the Swedish National Monitoring Programme while stations in blue are additional stations sampled by SMHI.

The Arkona Basin is the first basin that new deepwater flowing into the Baltic proper encounters after having crossed the entrance sills in Öresund and Fehmarn Belt (Figure 3). The deepwater flows along the bottom as a gravity-forced dense bottom current that mixes with resident Baltic surface water. The salinity of the inflowing deepwater therefore decreases as the flow proceeds into the basin and at the same time the volume flow increases (see Figure 4, showing flow of deepwater of various salinity at the entrance sills and just upstream the Bornholm Channel). Water entering through Öresund may have a salinity of 30 psu but the highest salinity of the deepest water in the East Gotland Basin varies around 13 psu. The change in salinity along the path is demonstrated in Figure 5.

Dense bottom currents coming from Öresund and Fehmarn Belt replenish a deepwater pool in the Arkona Sea that loses water by the dense bottom current carrying water through the Bornholm Strait and into the Bornholm Basin (see Figure 6). A deepwater pool is built up in the Bornholm Basin which is drained through the Stolpe Channel. This water sustains the deepwater in the large basins in the interior of the Baltic Proper.

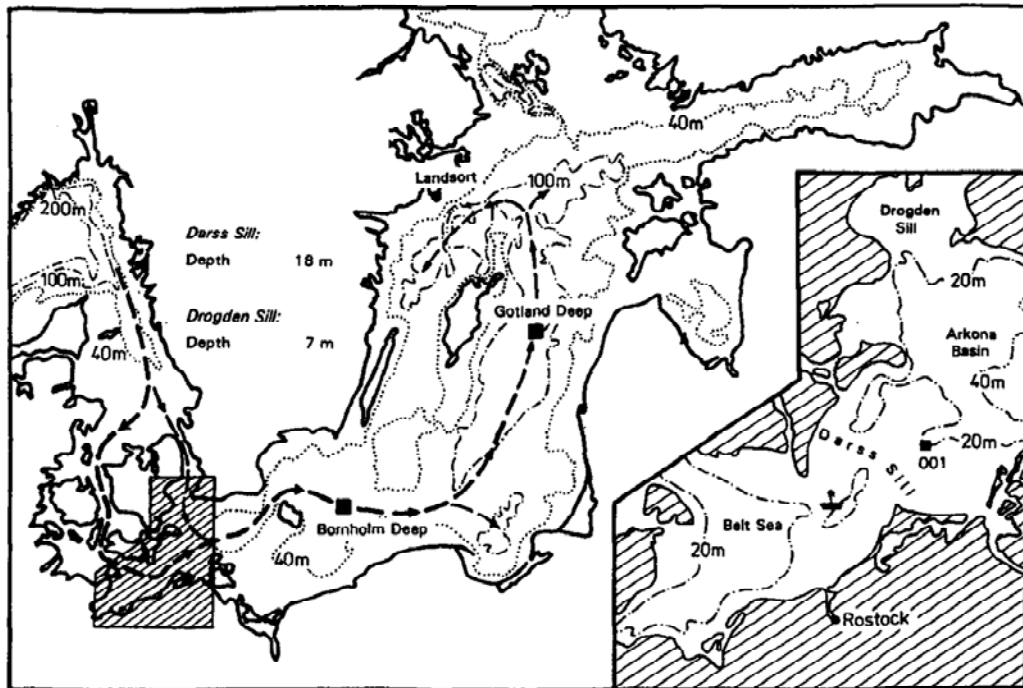


Figure 3. Map showing the topographic features of the Baltic Proper. Inserted is also the main path of inflowing deepwater. (From Matthäus and Lass, 1994.)

Only the largest and saltiest inflows may penetrate into the deepest parts of the large basins in the interior of the Baltic Proper. In periods with no large inflows the moderately salty new deepwater is interleaved in and just below the halocline in the deep basins of the Baltic Proper. During such periods anoxia develops in the deepest parts while the halocline area is well ventilated. In a decadal period ending in 1993, wintertime erosion of deepwater into the surface layer, above the halocline, was extremely strong in the East Gotland Basin whereby the top of the halocline sank from its usual position at about 60 m depth to 90 m depth. Such a large decrease of the volume of deepwater had not earlier been observed in the salinity record that starts in the 1890's. The oxygen conditions improved in the depth interval from about 80 to 120 m. As a consequence a large amount of phosphorus was deposited on the bottoms in this depth interval which led to a strong reduction of phosphorus in the surface water (Conley et al., 2003; Stigebrandt and Gustafsson, 2007). This in turn led to reduced biological production and there were no strong summer blooms of cyanobacteria.

Dense bottom currents entrain ambient water from above themselves. In the Bornholm Basin, there is always a gradient of upward increasing oxygen concentration in the depth interval where the dense bottom currents usually run, i.e. from 70 m depth to the top of the halocline at 40-50 m depth (see Appendix A). The water mixed into a dense bottom current will therefore contribute to increased oxygen transport by the current. The deepwater in the basins of the Baltic proper obtains oxygen mainly by the new deepwater. If the supply of deepwater increases due to increased mixing in the Bornholm Basin there will also be an increased oxygen supply to these basins.

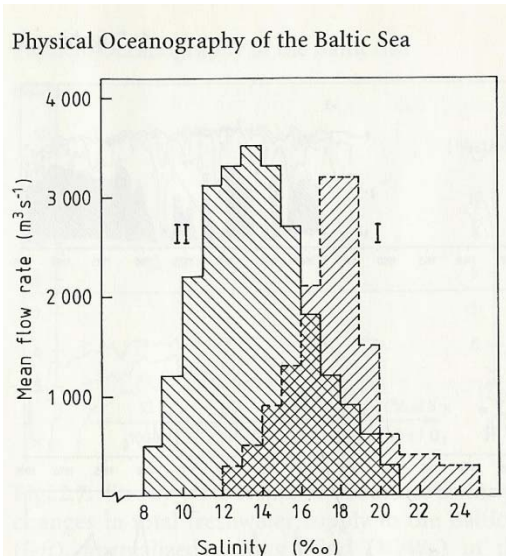


Figure 4. Distribution of flows into the Baltic Sea among different salinities at entrance sills (I) and in the Arkona Sea (II) respectively. Distribution I is a smoothed version of model computations (Stigebrandt, 1983) and II is a slightly smoothed version of a distribution computed from hydrographical data (Stigebrandt, 1987b). (From Stigebrandt, 2001)

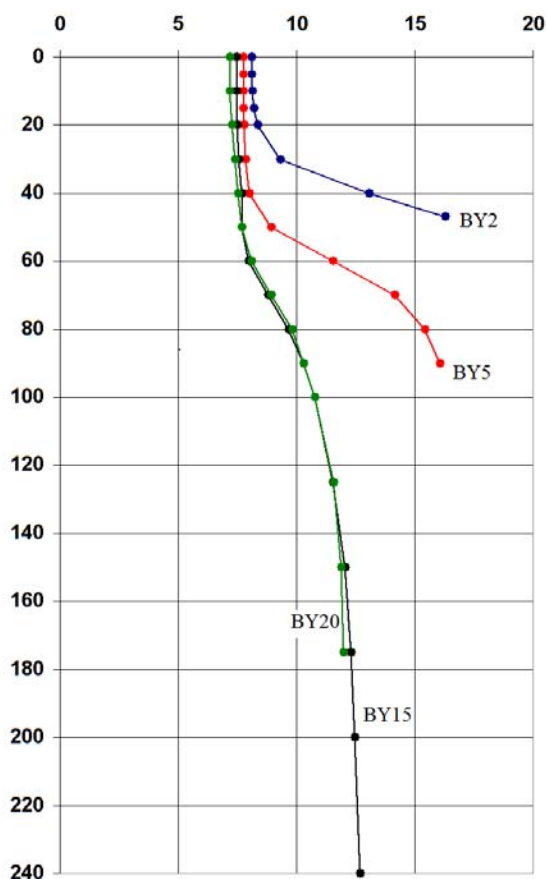


Figure 5. Salinity profiles (psu), based on climatological data presented in Appendix A, roughly along the pathway of deep water inflow. Station BY2 is located in the Arkona Basin, BY5 in the Bornholm Basin and, BY15 and BY20 in the Baltic Proper (Figure 2).

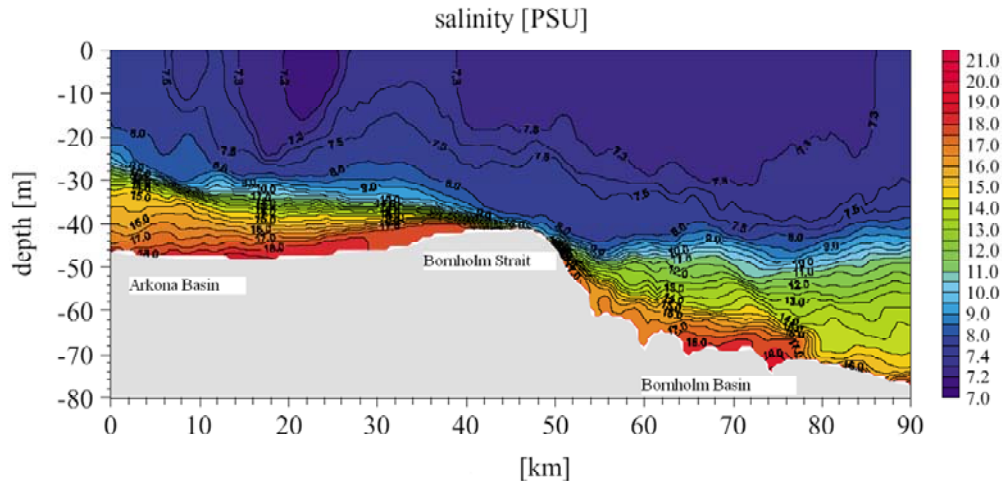


Figure 6. Salinity along a section from the Arkona Basin to the Bornholm Basin, passing the Bornholm Strait in February 2003. (From Piechura and Beszyńska-Möller, 2003.)

## 4 Currents in the western part of the Baltic Sea

In this chapter we try to synthesize, from observations and model results, some typical properties of currents and density stratification near the bottom in the western part of the Baltic Sea.

### 4.1 General description

Currents in the sea are forced in many ways due to adjustment to local and regional effects of wind forcing and density differences. Inertial and internal waves are generally occurring responses that may have different amplitudes in different areas due to differences in vertical stratification and water depth. Barotropic seiches are dependent on the specific topography of the basin. In the Arkona and Bornholm Basins there is a strong specific component due to the water exchange between Kattegat and the Baltic proper that causes strong temporary currents of new deepwater along the bottom in the Arkona Basin, and in the Bornholm Strait (Figure 8).

### 4.2 Observed bottom currents

A number of measurements of the bottom currents in the basins and straits of the western part of the Baltic Sea have been carried out during the last 35 years. Many of these observations have been collected during expeditions of limited duration but some long-term time series have become available during the last couple of years. Below some results from field observations have been gathered for each of the different areas.

**Arkona Basin:** As a part of the German MarNet Monitoring Network the automated station Arkonabecken (see Figure 7) has been measuring the currents throughout the water column since July 2006. The mean speed obtained at 40 m depth for the period July 2006 to August 2007 was 0.11 m/s with a standard deviation of 0.06 m/s. The maximum measured speed during this period was 0.31 m/s (A. Gyldenfeldt, BSH, pers. comm.).

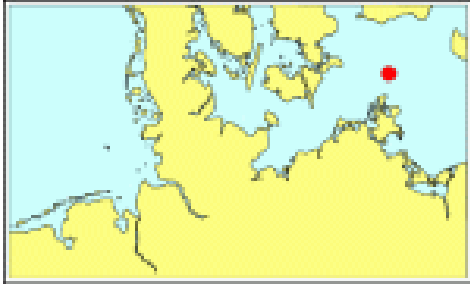


*Figure 7. Position of the German MarNet station Arkonabecken.*

Shortly after the large 1993 inflow a survey was undertaken in the Arkona Basin which gave a nearly synoptic picture of the hydrographic conditions and the current field (Liljebladh and Stigebrandt, 1996). Measurements were taken along six transects, covering the area from the central part of the basin to the Bornholm Strait. The current field was very complex as demonstrated in *Figure 8*, with maximum velocities being around 0.3 m/s. A dense bottom pool was found with the largest velocities encountered near its northern edge where the pycnocline hits the bottom. This picture becomes more clear when barotropic currents are removed and from geostrophic computations based on the observed vertical stratification (Liljebladh and Stigebrandt, 1996).

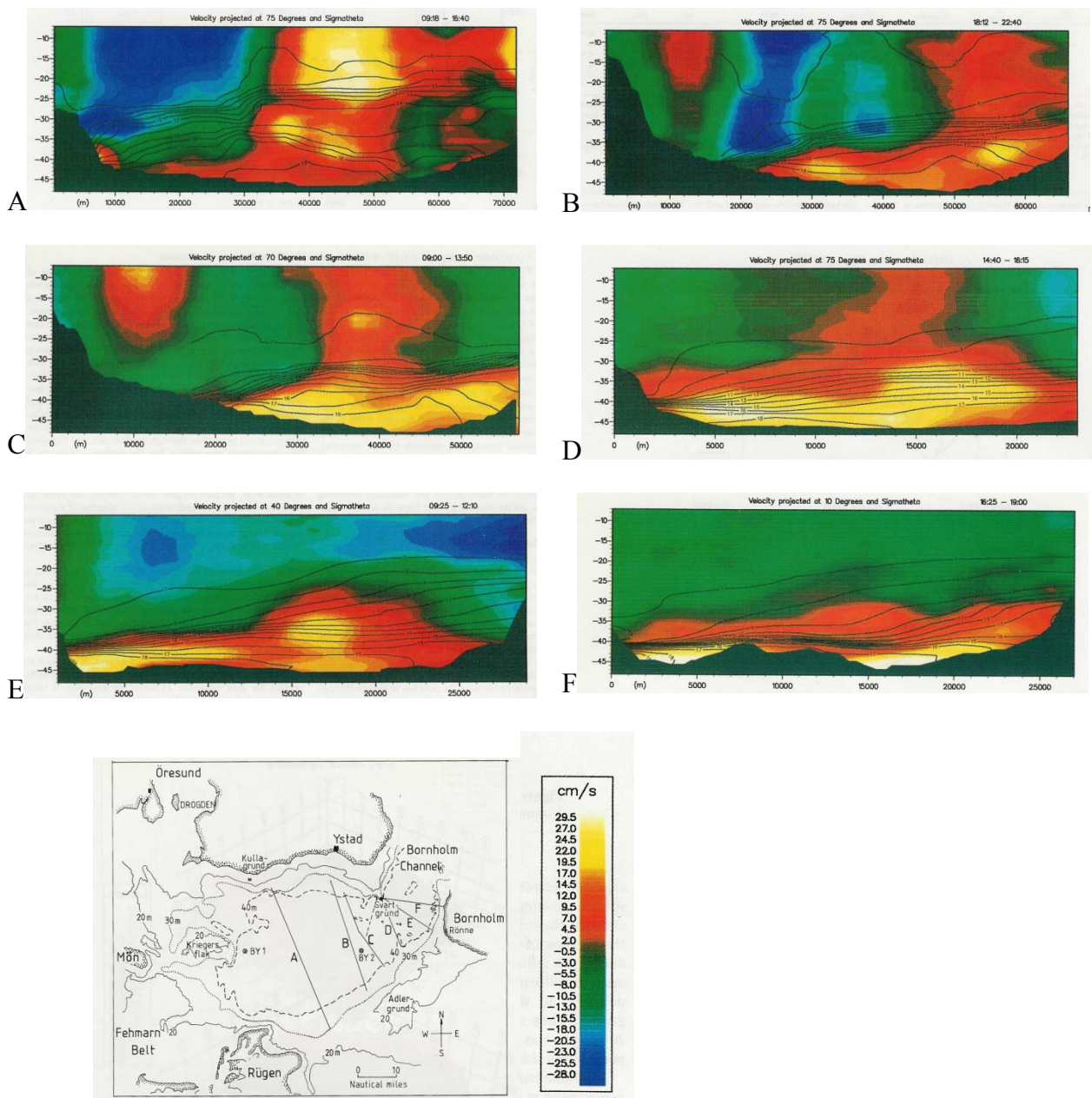
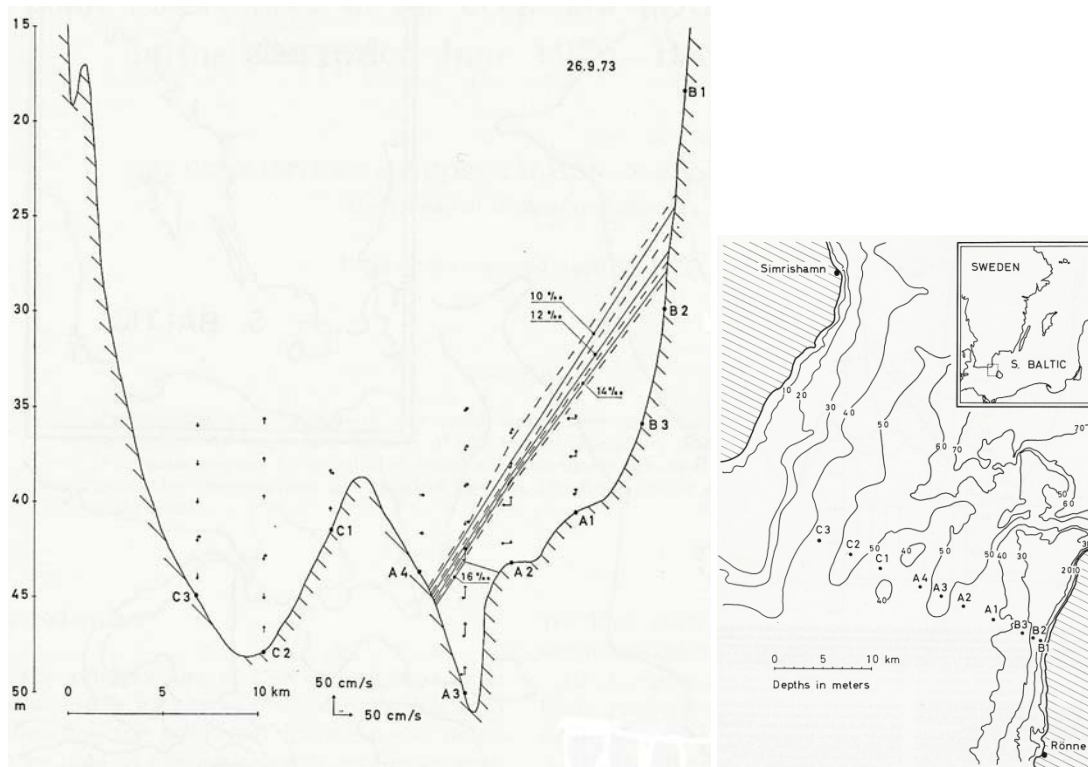


Figure 8. Current speed (in colours, positive values represent inflows) and salinity (isohalines) obtained from ship ADCP and CTD, respectively, in 6 different vertical sections (A-F, see the map) in the Arkona Basin and Bornholm Strait in February 6-7, 1993. (From Liljebladh and Stigebrandt, 1996).

The Polish Institute of Oceanology carried out 7 surveys in the western Baltic between December 2002 and August 2003, covering the very cold January inflow this year (Piechura and Beszyńska-Möller, 2003). In the Arkona a basin-wide cyclonic circulation was found.

**Bornholm Strait:** The Bornholm Strait, which connects the Arkona Basin and the Bornholm Basin, has a sill depth of 47.3 m according to the Swedish Water Archive (SMHI, 2003). The section at which the flow experiences the maximal constraint is

not unambiguously defined, but should be close to the section shown in the right panel in *Figure 9*. From June 1973 to December 1974 a total of 17 transects were conducted across this section with detailed measurements of the currents carried out (Petrén & Walin, 1976; Rydberg, 1980). The dense inflow from the Arkona Basin to the Bornholm Basin was mainly, but not exclusively, through the southeastern channel of the Bornholm Strait. For the transect shown in *Figure 9* high-saline water was only found in the southeastern channel. The maximum velocities of the inflowing water were typically  $\leq 0.5$  m/s during the time period of the study. It may be noted that the well-mixed layer beneath the halocline is several meters thick (*Figure 9*).



*Figure 9.* A section across the Bornholm Strait (Sweden to the left) showing isohalines and current components (upward arrows are into the Baltic). The location of the cross-section is shown in the right panel. (From Petrén and Walin, 1976).

The Polish ADCP-measurements across the Bornholm Strait after the 2003 inflow yielded speeds of the dense water of around 0.3 m/s. In January the inflow took place in both channels while a month later the dense water was pushed up on to the southeastern slope (Piechura and Beszyńska-Möller, 2003).

**Rügen-Adlergrund:** The main passage for deep water transport between the Arkona Basin and the Bornholm Basin is the Bornholm Strait. However, when the deep-water pool is thick enough in the Arkona Basin some water may spill over the sill between Rügen and Adlergrund, which has a depth of 28 m. Lass et al. (2001) reported on current observations from a section across this passage. An inflow with enhanced salinity was observed close to Rügen with currents in the range of 0.05-0.1 m/s. At a section further downstream (Oderbank-Adlergrund) no deep-water inflow was detected. From hydrographic measurements obtained at the hydrographic station BY1 (see *Figure 2*) in the Arkona Basin, Stigebrandt (1987b) estimated that about



10% of the total volume flow of new deepwater should take the route between Rügen and Adlergrund. Most of the flow should occur during peaks of major inflows. This estimate was made for a sill depth of 30 m and should therefore be an overestimation.

**Bornholm Basin:** From geomorphological investigations in the western part of the Bornholm Basin interesting conclusion can be made about the bottom currents. In Sivkov and Sviridov (1994) a map was presented showing the pathways of the near-bottom currents in the area (*Figure 10*). The two channels in the Bornholm Strait present bottom features indicating that the largest velocities are found here. Several pathways for the bottom water were found, after entering the Bornholm Basin, most of them going in a south-easterly direction moving the water towards the southern flank of the Bornholm Basin. By distinguishing between symmetric and asymmetric erosional-accumulative forms the authors could identify areas dominated by fast, gravitational currents and areas where slower, geostrophic currents dominate. This might mirror a dependence on the buoyancy of the currents, with slower currents in areas where the gravitational forcing has disappeared and the water has been interleaved at neutral buoyancy. From *Figure 10* one should expect relatively slow currents along the pipeline section.

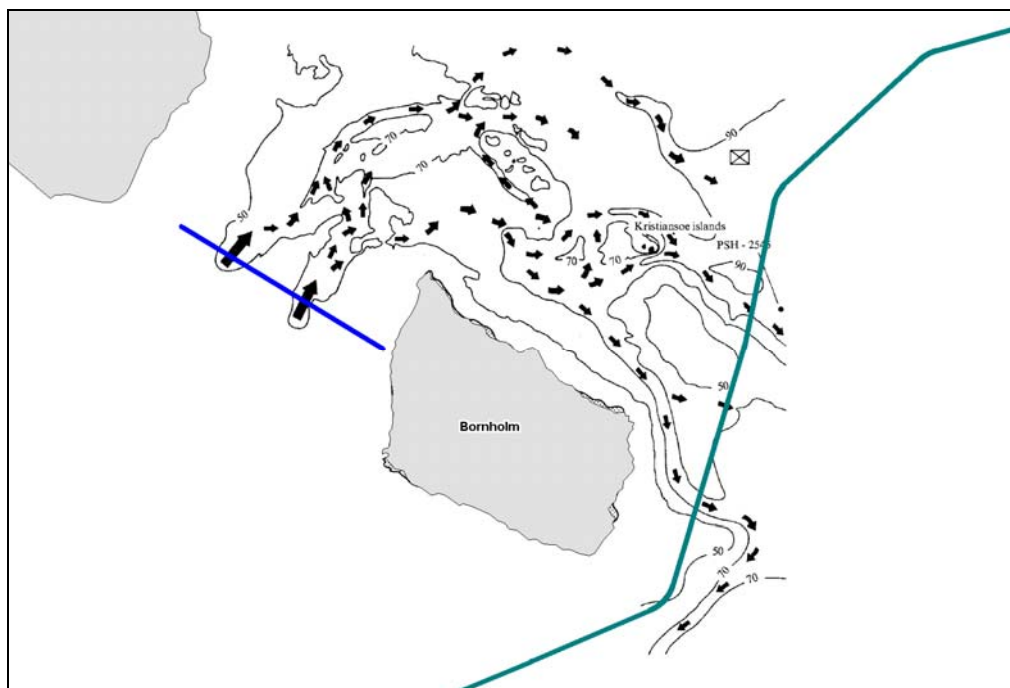


*Figure 10. Pathways of nearbottom currents (from geomorphological data). Inserted are the location of the pipeline route and the cross-section shown in Figure 9. (Adapted from Sivkov & Sviridov, 1994).*

From the January 2003 survey Piechura and Beszyńska-Möller (2003) report that the measured near bottom velocity of the water entering the basin along the southern edge was up to 0.75 m/s. The hydrographic observations and the current field at 50 m suggested a cyclonic circulation in the Bornholm Basin (see *Figure 11*). When the dense bottom current meandered along the southern slope baroclinic eddies were

developed. It was furthermore concluded that for the 2003 inflow the Bornholm Basin was the main area for mixing.

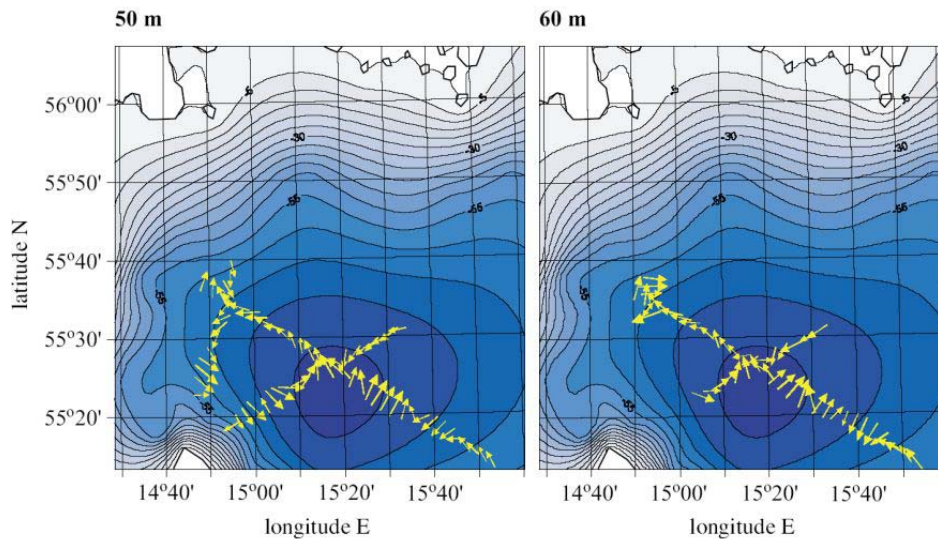


Figure 11. Currents at 50 and 60 m depth obtained from Polish ADCP measurements in January 2003 (Piechura and Beszyńska-Möller, 2003).

**Stolpe Channel:** During one week in August 1976 daily current measurements were carried out across two sections in the Stolpe Channel (Rydberg, 1976) which has a sill depth of around 60 m. The maximum along-channel velocity in the 10-m thick layer closest to the bottom was 0.5 m/s in the western section (close to the sill) while the values were lower at the eastern section of the channel.

In April-June 1993 continuous current measurements were undertaken by SMHI in the Stolpe Channel. On the southern side of the channel at 65 m depth the maximum current speed amounted to 0.6 m/s (B. Broman, SMHI, pers. comm.) According to Piechura and Beszyńska-Möller (2003) the speed of the dense bottom currents in the Stolpe Channel amounted to 0.2-0.3 m/s in January and April 2003.

### 4.3 Modeled currents

From model runs carried out at DHI using the Mike 3 model (<http://www.dhigroup.com/Software/Marine/MIKE3.aspx>) bottom currents for the period 2004-01-01 to 2008-10-31 have been obtained. The horizontal and vertical resolution of the model is 1 nm and 1 m, respectively, and data output is provided every 30 minute. In Figure 12 the spatial distribution, size and frequency of the bottom currents are presented for seven positions in the Arkona and Bornholm Basins. Along the proposed route the velocities are generally very low and aligned in the northeast/southwest or east/west direction (Figure 12b). The bottom velocities are higher for the three positions denoted NS, NN1 and NN2 (Figure 12c). The highest velocities (0.1-0.2 m/s) are found on the northern side of the Bornholm Basin going in either a westerly direction or in an easterly/south-easterly direction. At the north-eastern rim of the Bornholm Basin the NE site is where a possible flow along the edge, and above the sill depth of the Stolpe Channel, crosses the route of the pipelines. For this location the bottom velocities are also very low and no preferred direction can be identified.

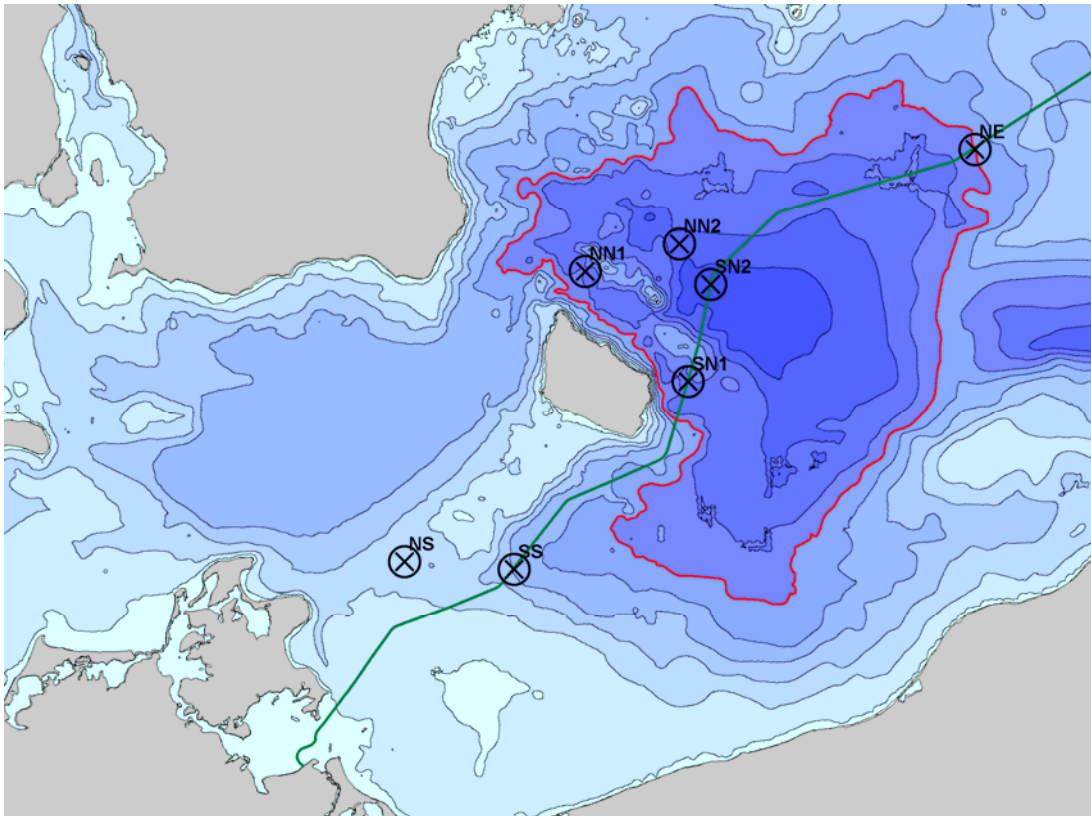


*Figure 12a. Positions at which model data have been extracted. The green line shows the proposed route while the dark red line indicates the alternative route. The thinner red line is the depth contour for the Stolpe Channel sill depth.*

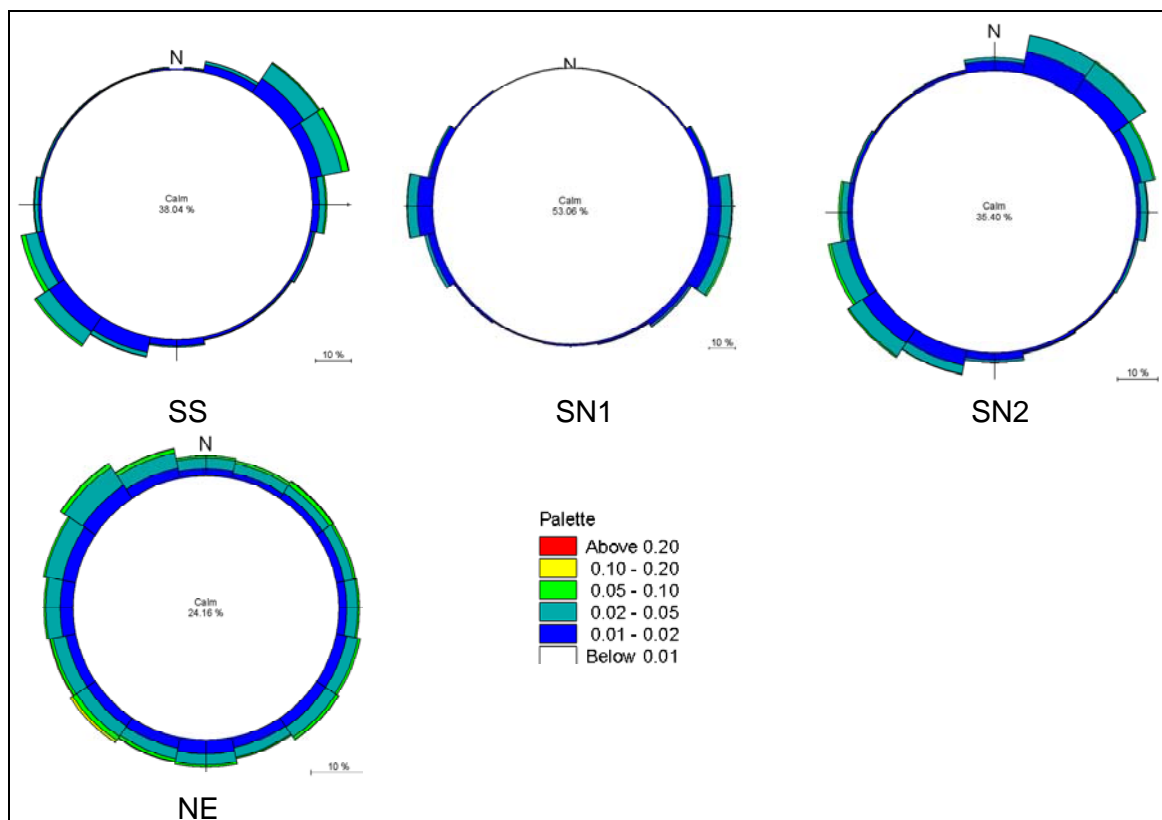


Figure 12b. Current roses for the bottom layer at different positions along the proposed southern route (see map above), obtained from the MIKE 3 model. (Model data have been provided by Ramböll.)

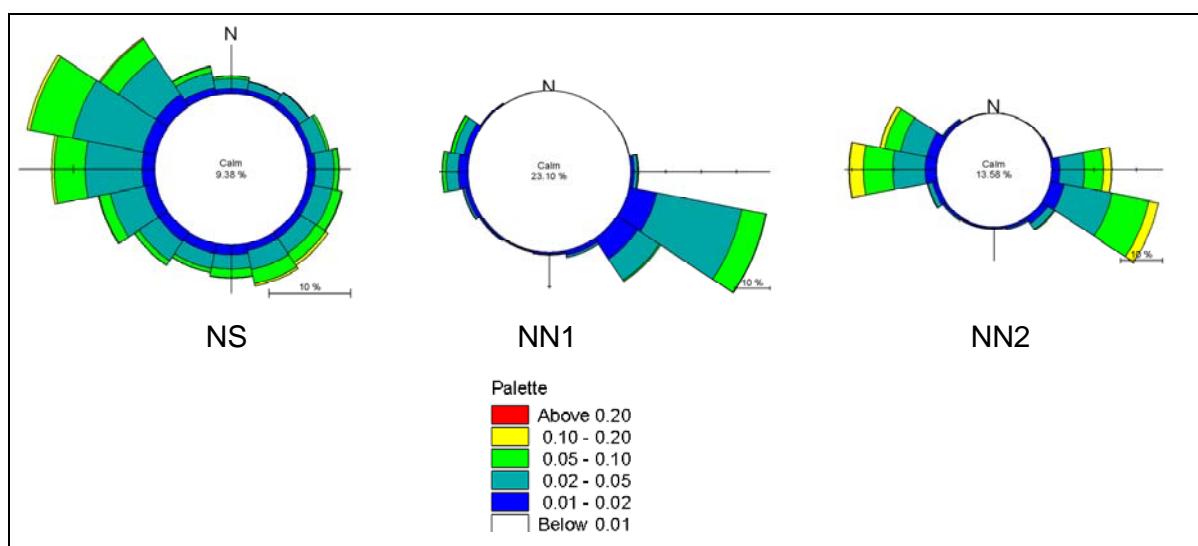


Figure 12c. Current roses for the bottom layer at different positions in the Arkona and Bornholm Basins (see map above), obtained from the MIKE 3 model. (Model data have been provided by Ramböll.)

Within the QuantAS project the bottom salinity in the Arkona Basin was modeled for a period of 9 months and a movie (presented on the web-site <http://www.io->

warnemuende.de/quantas/index.php) was produced for this time period. One may deduct from the model results that during these 9 months 4 overflows with enhanced salinity took place over the Rügen-Adlergrund ridge. The main transport of saline deep water went, however, at these occasions through the Bornholm Strait. This overall impression from the model results corresponds well to the conclusion based on hydrographical observations at BY1 reported in Stigebrandt (1987b), mentioned above under the heading Rügen - Adlergrund.

#### 4.4 Density stratification close to the bottom

Both the flow resistance (form drag) by the pipelines acting on a crossing current, and the structure of the resulting turbulence, depend on the local vertical stratification in the crossing section (Appendix C). If the water is vertically homogeneous, the form drag causes eddies in the current downstream of the pipelines but there is no extra mixing due to the pipelines. However, if the water is vertically stratified close to the bottom and the speed of the crossing current is less than the speed of internal waves (waves in the stratification), the flow resistance by the pipeline takes the form of internal waves that may transfer energy from the current into the stratification. To estimate the flow resistance and the resulting mixing we have investigated the vertical structure of the density field close to the bottom in the Bornholm Basin as discussed below.

Around 240 CTD profiles from stations in the Bornholm Basin, with a bottom depth in the range of 40-70 m, were investigated. In many cases the profiles did not extend all the way to the bottom, but for 46 profiles it was possible to judge whether there was a homogeneous bottom layer present or if the layer below the halocline was stratified all the way to the bottom. A mixed bottom layer was found in 27 profiles for which the velocity  $c_i$  of the lowest internal wave mode was calculated. It was found that the mean value of  $c_i$  was 0.55 m/s with a standard deviation of 0.18 m/s. A similar calculation was also carried out for the stratified bottom layer giving  $c_i = (0.4 \pm 0.14)$  m/s. The reduced gravity,  $g'$ , for the 46 profiles was furthermore determined to  $(3.4 \pm 1.6) \times 10^{-2} \text{ ms}^{-2}$ .

## 5 The Gotland Sea

The hydrography of the Gotland Sea was touched upon in Chapter 3 with references also to Appendix A where vertical profiles of the observed temperature, salinity, density and oxygen are provided for the Gotland Deep (BY15) and the Fårö Deep (BY20). The deepwater entering the Gotland Basin continues towards the Gotland Deep (249 m) and then further into the Fårö Deep (205 m). The sill separating these two basins is 140 m deep. North of the Fårö Deep the flow divides into two branches, one going into the Gulf of Finland and the other one continuing towards the Landsort Deep. In *Figure 13* the approximate path of the inflowing water is shown.

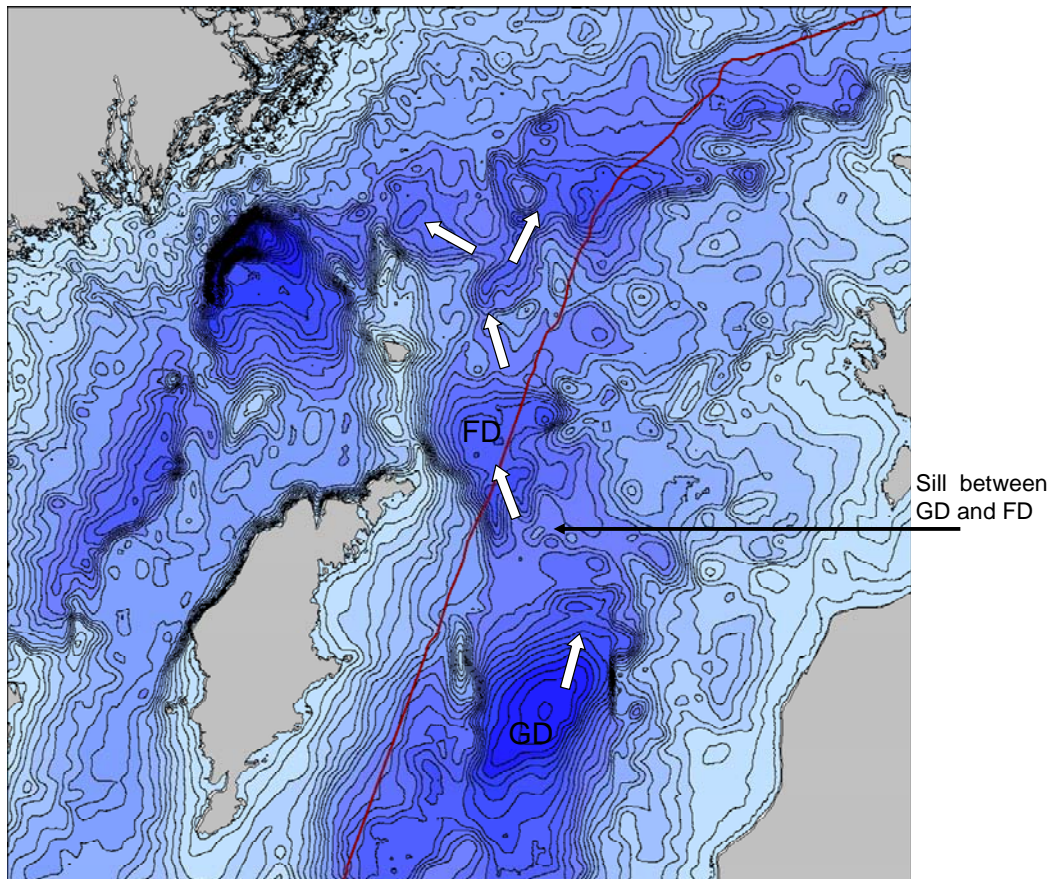


Figure 13. Detailed bathymetry of the East and North Gotland Sea with the route of the pipelines shown in red. The approximate path of the deep water is indicated by the arrows. GD - Gotland Deep, FD - Fårö Deep.

Long-term time series of observed deepwater currents in this area are, to our knowledge, scarce. A complication is the presence of hydrogen sulphide below the perennial pycnocline which requires special mooring techniques. A 3-year long record of currents is, however, available from the north-eastern part of the Gotland Basin (Hagen and Feistel, 2004), see *Figure 14* for position. Measurements were obtained at 204 m depth, 20 m above the seabed, from August 1999 to October 2002. The mean velocity in the along-slope (north/south) direction was 0.03 m/s to the north with a standard deviation of 0.0003 m/s. The highest velocity recorded in this direction during the 3-year period was 0.4 m/s. The mean of the cross-slope velocity was close to zero.

From model runs carried out at DHI using the Mike 3 model, bottom currents for the period 2004-01-01 to 2008-10-31 have been obtained for a position where the pipelines crosses the Fårö Deep (see *Figure 14*). The horizontal and vertical resolution of the model in the Gotland Sea is 3 nm and 1 m, respectively, and data output is provided every 30 minute. The spatial distribution, size and frequency of the bottom currents are presented in *Figure 15*. The velocities are very small and directed towards northwest or southeast. The size of the mean currents is comparable with those observed in the Gotland Basin.

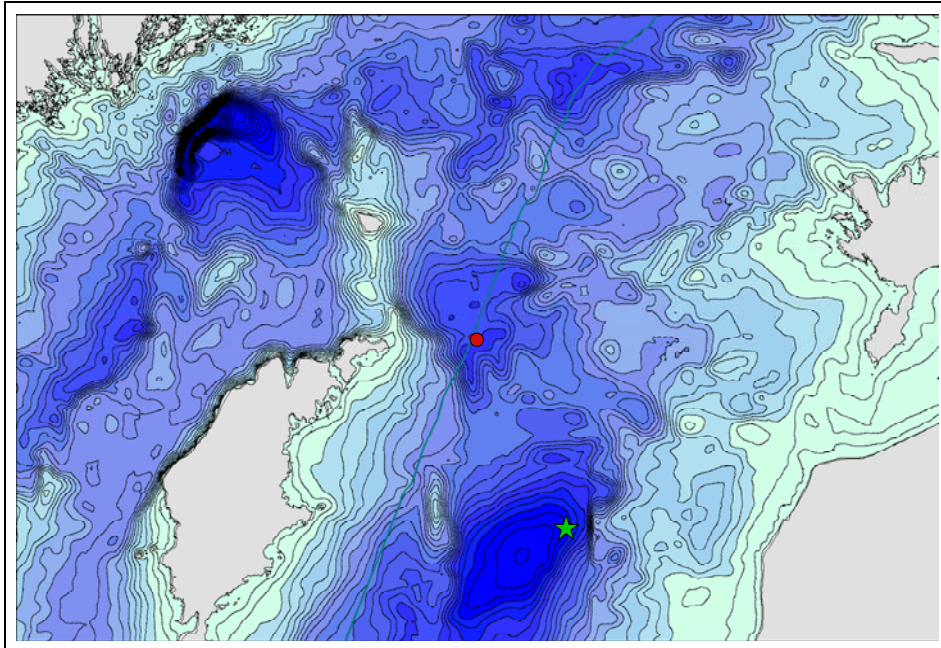


Figure 14. Map showing the position of observed currents (green star) and the position at which model data have been extracted (red dot). The green line shows the proposed route.

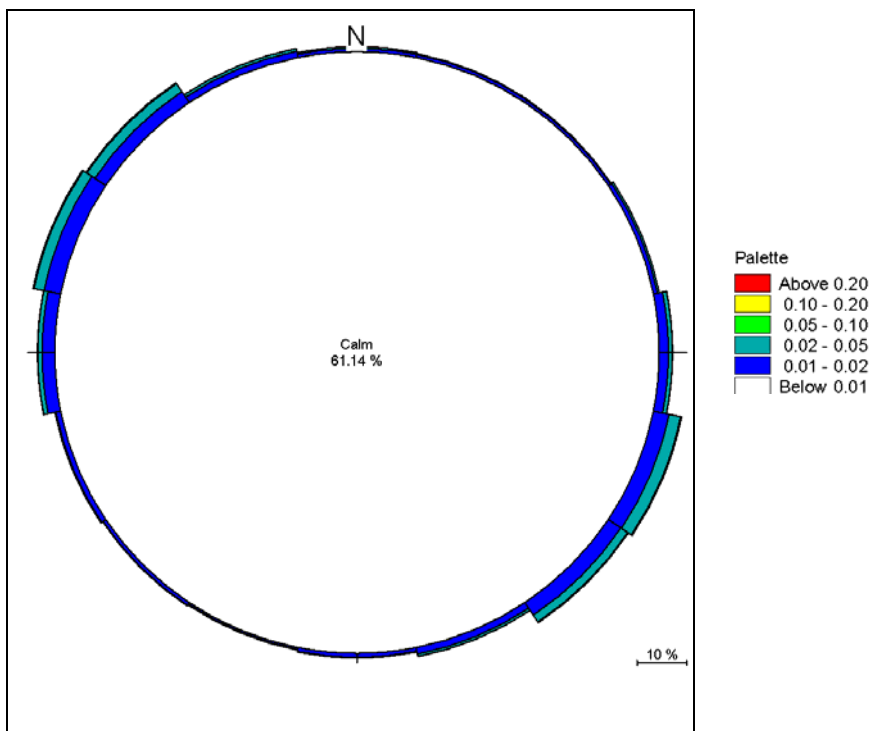
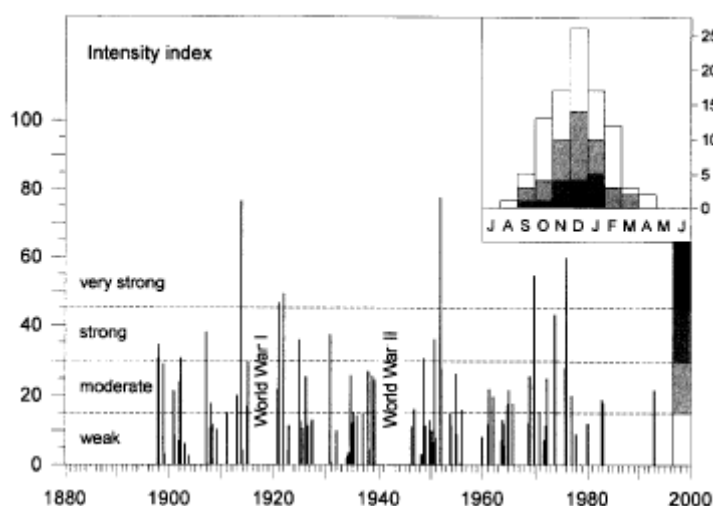


Figure 15. Current rose for the bottom layer in the Fårö Deep, obtained from the MIKE 3 model. (Model data have been provided by Ramböll.)

## 6 Properties of water exchange

Inflow of new deepwater occurs when, for a period of days, the sea level stands higher in Kattegat than in the south-western Baltic. The inflow for a given sea level difference depends on the resistance properties of the straits between Kattegat and Arkona Sea. Using the daily mean sea level in Kattegat and the freshwater supply to the Baltic Sea, the barotropic water exchange through the entrance straits and the horizontal mean sea level in the Baltic may be modeled quite well, Stigebrandt (1980) and e.g. Gustafsson and Andersson (2001). The latter authors showed that sea level variations longer than about 15 days in Kattegat can be modeled from the west-east wind over the North Sea which may be estimated from the north-south atmospheric pressure difference estimated from observations at Oksøy and de Bilt.

The largest occurring inflow events raise the sea level in the Baltic by about 1 meter in a couple of weeks which implies an accumulated inflow of about 350 km<sup>3</sup>. Statistically, such large inflows occur only about once a decade as illustrated in *Figure 16*. Most inflows are much smaller; see e.g. Matthäus and Franck (1992) and Gustafsson and Andersson (2001). During an inflow event the salinity of new deepwater increases with time as the storage of freshwater in the surface waters of the Belt Sea and Kattegat decreases. Inflow statistics based on hydrographical measurements at BY1 (for location see *Figure 2*) in the Arkona Basin show that larger inflows are saltier than smaller inflows (e.g. Stigebrandt, 1987b). Stigebrandt (1983) showed that simple coupled two-layer models of Kattegat and the Belt Sea, that describe the salinity gradients in the entrance area, together with the barotropic model mentioned above can be used to compute the salt exchange between Kattegat and the Baltic. Gustafsson and Andersson (2001) showed that even a simple regression model of the horizontal salinity gradient in Kattegat and the Belt Sea does a decent job. Using their model, these authors computed the salt fluxes for all major inflows to the Baltic Sea from 1902 to 1998 (*Figure 17*). Their ranking of the largest inflows compares rather well to a ranking based only on volume flows by Fischer and Matthäus (1996).



*Figure 16. Major Baltic inflows and their seasonal distribution (inset) characterized by an intensity index. (From Schinke and Matthäus, 1998).*



The results of Gustafsson and Andersson (2001) support the conclusions drawn in Stigebrandt (1983) that the exchanges of water and salt between the Kattegat and Baltic Proper are independent of the vertical stratification in the south-western Baltic Sea. There is essentially no upstream influence from the conditions in the Arkona and Bornholm Seas on the inflow of new deepwater to the Baltic Proper. However, very strong winds over the Arkona Sea may create thick well-mixed surface layers that erode new deepwater stored in the basin as discussed in Liljebladh and Stigebrandt (1996) and Gustafsson and Andersson (2001). Such a case occurred for instance in January 1990 when very strong winds homogenized the whole water column in the Arkona Basin whereby the salinity of the surface water increased from about 8 psu to 11 psu. This was, however, an exceptional event when the wind speed was far from its mean value. The properties of the regional wind, here represented by the conditions at Falsterbo, are shown in Appendix B.

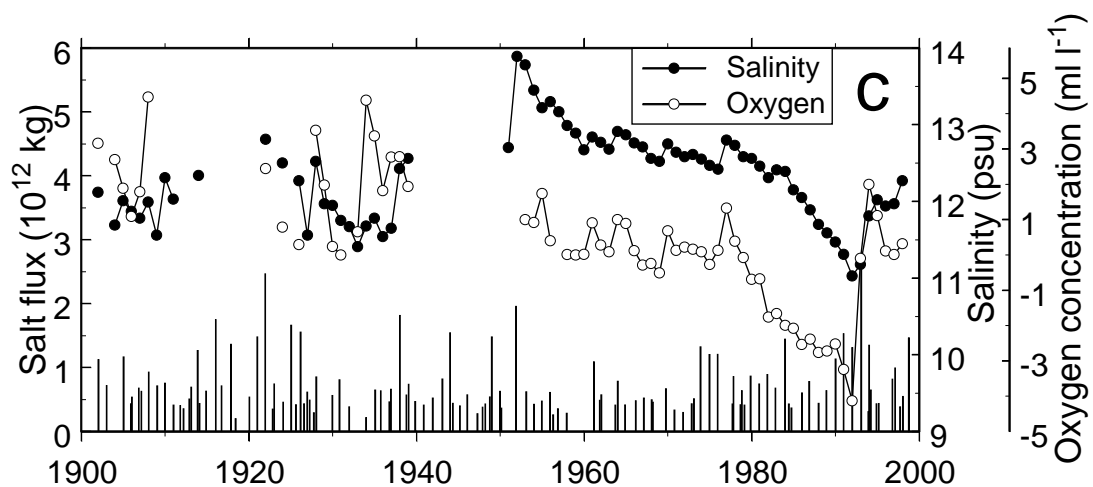


Figure 17. Computation of the integrated salt flux in major inflows (staples). Also shown are salinity and oxygen at 200 m depth in the east Gotland Basin. (Gustafsson and Andersson, 2001, their figure 15).

## 7 Dynamics of the deepwater flow

This chapter describes dynamical processes that are of importance to the flow of deepwater in the Baltic Proper.

### 7.1 Frictional flow and mixing

Instabilities of various kinds transfer energy from currents to turbulence. Most of the turbulent energy is dissipated to heat but a small fraction (expressed by the flux Richardson number –  $R_f$ ) is used for diapycnal mixing. Mixing efficiency is defined as  $R_f/(1-R_f)$ . Bottom and interfacial stresses acting on dense gravity currents generate turbulence and all turbulence in the new deepwater may contribute to mixing between the new deepwater and residing water above. Pipelines crossing the route of the new deepwater will impose non-viscous drag on the current which, for weak stratification manifests itself as eddies downstream of the pipelines or, for stronger stratification, internal lee-waves. This is of immediate interest because turbulence generated by lee-waves might have higher  $R_f$ -value, and thus higher mixing efficiency, than turbulence due to bottom and interfacial stresses (see

Appendix C). If so, the new deepwater will be slightly more mixed than at present due to the pipelines.

Dense gravity currents are driven by their excess buoyancy relative to the ambient water. The potential energy of new deepwater when it passes the entrance sills, relative to the residing pool of deepwater is spent to drive the current against frictional forces so the energy is transformed to turbulent energy. This was utilized in a model of a dense bottom current developed by Stigebrandt (1987a), see Appendix C. For a given flow the model shows that the entrainment of overlying ambient water is proportional to  $W^{2/3}Rf$  where  $W$  is the width of the current. The width is known only in narrow systems, see an application to the Gullmar Fjord in Arneborg et al. (2004), and in basins with narrow canyons where the current runs. In applications of the model to the Baltic the width of the current is tuned; e.g. Stigebrandt (1987a), Omstedt and Axell (2003) and Gustafsson (2003).

The potential energy of new deepwater when crossing the entrance sills in Fehmarn Belt and Öresund is lost to turbulence generated by bottom and interfacial friction. Of this 4% is used for diapycnal mixing while 96% is dissipated to heat, thus  $Rf=0.04$  (Appendix C). The reason for the low mixing efficiency of dense bottom currents is probably that the turbulence is mainly generated near the sea bed by bottom friction where water is more or less well-mixed. Turbulence acting in the stratified water closer to or at the interface to the ambient water above might be more efficient in performing diapycnal mixing. For our computations we also use  $Rf=0.12$  to get a conservative highest estimate of the mixing effect, see Appendix C.

## 7.2 Hydraulic flow and upstream influence

A change in the cross-section area of a strait or at a sill could lead to altering upstream conditions which would affect the overflow. Deep-water flows through straits and over sills may sometimes be determined just by knowing the upstream thickness of the bottom layer, the density difference between the upper and lower layer and the geometry of the constriction. Estimates of the maximum flow capacity are then achieved by applying the concept of rotating hydraulics for an inviscid flow (Whitehead et al., 1974., Rydberg, 1980, Borenäs and Lundberg, 1986). It is reasonable to assume that if the bottom layer is not too shallow in the upstream basin friction may here play a limited role. This is in contrast to what is found for the descending overflow plume on the downstream side of the sill.

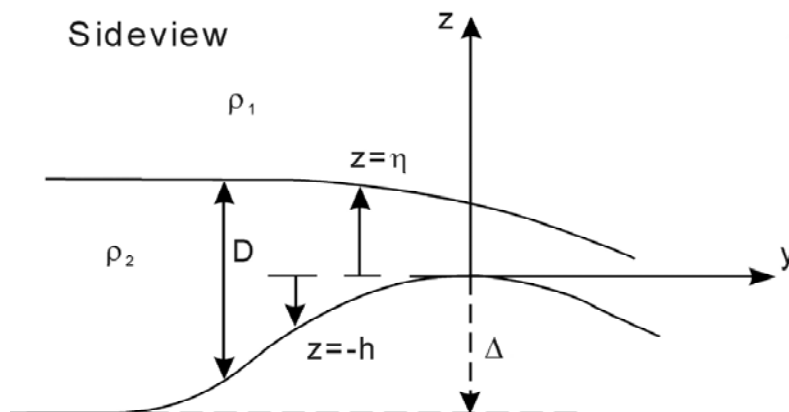


Figure 18. Sketch showing the position of the interface between the bottom layer of density  $\rho_2$  and the upper layer of density  $\rho_1$  along a channel with a sill height  $\Delta$ .

The hydraulic theory is often applied to situations when the depth of the interface drops from the upstream side of the sill to the downstream side. For an inviscid flow the upstream and downstream level can in this case only be connected if the flow at the top of the sill is critical, which means that the flow velocity has to equal the speed of a long wave. The flow is then maximized and the sill controls the upstream height of the interface. There are two approaches that will be discussed,

1. in the first case the flow is locally controlled with regard to an internal long wave.
2. in the second case the flow is on average controlled by a rotating internal long wave.

For a simplified geometry, with the cross-channel geometry approximated by a rectangular, the modeled velocity distribution at the control section differs between the two cases. For the locally controlled flow the velocity is highest on the right hand side (looking in the downstream direction) while for the second case the maximum velocity is found at the left-hand edge of the flow. For both cases (and assuming that the depth of the bottom layer in the upstream basin is much larger than depth of this layer at the top of the sill) the maximum flow rate through the channel is proportional to the square of the upstream height,  $\eta_{\infty}$ , of the interface above the sill level (see *Figure 18*).

The concept of rotating hydraulic flow is based on the assumption of steady state and that the frictional effects are negligible compared to the inertial, conditions which are generally not satisfied in the western part of the Baltic proper. However, during periods of major deep-water inflows the Arkona and Bornholm basins may have large and comparatively steady pools of deep water, and at these occasions the hydraulic theory may be justified. This was also concluded by Borenäs et al. (2007) who investigated whether the flow through the Stolpe Channel is hydraulically controlled with regard to a rotating internal wave.

According to observations the flow between the Arkona Basin and the Bornholm Basin is usually larger in the southeastern channel than in the northwestern (Petrén and Walin, 1976, Piechura and Beszyńska-Möller, 2003). When the theory for a locally controlled flow is used for the actual topography in the Bornholm Strait the maximum velocity is found in the deepest part of the southeastern channel, but the velocities on the Bornholm flank may be fairly high as well (Rydberg, 1980). If there is a deep-water flow through the northwestern channel the maximum velocity will be lower here than in the southeastern channel.

### **7.3 Topographic steering**

A dense current flowing along a sloping bottom may be subjected to topographic steering when encountering small-scale topographic features intersecting the slope. This effect has been investigated by, e.g., Darelius and Wåhlin (2007) who studied the steering effect of ridges and canyons on a geostrophic flow. They concluded that part of the flow will be channelled down the slope while the rest will continue over the obstacle. The size of the topographically steered geostrophic transport depends on the geometry of the obstacle, the slope of the bottom, the stratification and the thickness of the frictional Ekman layer.

## 8 Interaction between the flow of new deepwater and the pipelines

The pipelines may influence the deepwater of the Baltic Proper in three ways.

1. Firstly, pipeline-generated turbulence might be more efficient than turbulence generated by bottom and interfacial friction and this may increase the mixing between the new deepwater and ambient water.
2. Secondly, the pipelines may increase the sill height and thereby dam the dense deepwater if it is placed in a section of hydraulic control.
3. Thirdly, the pipelines may steer the dense water downslope if the current encounters the pipelines when flowing along a sloping bottom.

### 8.1 Frictional flow

First we investigate how much of the dissipation that the crossing pipelines might cause. The analysis is based on theory described in Appendix C. The total dissipation by the dense bottom current between the entrance sills and Stolpe Channel, where the outlet of dense water from the Bornholm Basin occurs, can be estimated as  $D_0=LWUS$  where  $L$  is the length,  $W$  the typical width and  $U$  the typical velocity of the dense bottom current.  $S$  is the bottom stress computed from  $S=\rho_0C_DU^2$ . Here  $C_D$  is the coefficient for combined bottom and interfacial drag and  $\rho_0$  is a standard density. The dissipation caused by the crossing pipeline of height  $h$  equals  $D_p=WUh\rho_0CU^2$  where  $C$  is the coefficient for drag caused by the pipeline and we have assumed that the width and speed of the current crossing the pipelines are equal to  $W$  and  $U$ , respectively. Typical value of  $C_D$  is 0.003 and a typical value of  $C$  equals 1.5, see Appendix C. This means that one pipeline of height  $h=1.0$  m exerts a drag equivalent to the frictional drag along a stretch of about 500 m. The ratio between the drag caused by two pipelines and the total drag equals  $R=2hC/(L C_D)$ . With the figures for  $h$ ,  $C_D$  and  $C$  given above and with  $L=200$  km one obtains  $R=0.005$  (=0.5%)

The increased mixing due to two pipelines equals  $\Delta M=R \cdot (R_{f_{\text{pipe}}}/R_f - 1)$ . Assuming that the mixing efficiency of form-drag generated turbulence were a factor of 3 greater than for turbulence generated by combined bottom and interfacial friction, i.e.  $R_{f_{\text{pipe}}}\approx 0.12$  and  $R_f\approx 0.04$ , one would get estimates of the highest possible mixing increase (c.f. Appendix C). From the formula above one finds that the total mixing of the new deepwater with ambient water in this case would increase by  $\Delta M=2R$  which equals about 1.0% for a 1.0 m high pipe. NB!  $\Delta M=0$  if  $R_{f_{\text{pipe}}}=R_f$ . If the speed and width of the current in the crossing section are less than  $U$  and  $W$ , respectively, the dissipation (and mixing) caused by the pipelines will be lower. According to Figure 12 the modeled bottom velocities are generally lower than 0.3 m/s. However, there is an uncertainty in how well the modeled bottom currents represent the true currents. Here we use  $U=0.3$  m/s as an upper limit.

It might be interesting to estimate  $D_0$  for the Arkona and Bornholm Basins. An alternate expression for  $D_0$  is given by Eq.(C11) based on the loss of potential energy of the new deepwater between the entrance sills and the Stolpe Channel, thus  $D_0=\rho_0Qg'h_1$ . Inserting the following values  $Q=15,000$  m<sup>3</sup>s<sup>-1</sup>,  $g'=0.06$  m s<sup>-2</sup>,  $h_1=60$  m, one obtains  $D_0=54$  MW. Using  $L=200$  km,  $W=10$  km,  $U=0.3$  ms<sup>-1</sup> and  $C_D=0.003$  in Eq. (C9) one obtains  $D_0=60$  MW. The typical width  $W=10$  km and the typical velocity  $U=0.3$  ms<sup>-1</sup> of the dense bottom current fits well with observations and

model results, see Chapter 4, and also give a quite realistic value of the dissipation. The values of  $Q$  and  $g'$  used here are the mean properties of new deepwater that may be obtained from conservation of flows of salt and water across the entrance sills.

The deepwater in the Arkona Basin has a short residence time so that turbulent mixing driven by wind and barotropic fluctuations should usually be small compared to mixing performed by the gravity current itself. Thus, mixing of Baltic Sea surface water and new deepwater should usually take place mainly in the gravity current. The estimates above are therefore quite relevant for the possible change of mixing of deepwater due to the pipelines.

The velocities in the Gotland Basin are lower than those in the Arkona and Bornholm Basins (see Chapters 4 and 5) and consequently the possible increase in mixing due to the pipelines should be less here.

## 8.2 Hydraulic flow

With the latest proposed route the pipelines will not pass any sills in the southwestern part of the Baltic Proper and, hence, the hydraulic considerations are not relevant here. In the Gotland Sea the pipelines will cross the path of the deep-water inflow in the Fårö Deep (see *Figure 13*) and they will not affect any sill flows.

## 8.3 Topographic steering

Topographic steering could possibly play a part if the dense flow crosses the pipelines on the slopes between Bornholm and the deeper part of the Bornholm Basin.

Consider a geostrophic flow along a sloping bottom as illustrated in *Figure 19*. When the flow encounters the pipelines a portion of it may be steered down the slope. To estimate the maximum size of the down-slope flow the pipelines may be treated as a small ridge intersecting the slope.

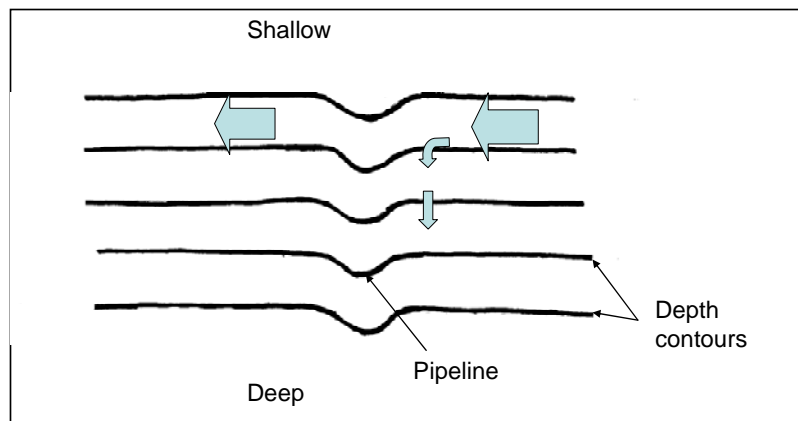


*Figure 19. Sketch showing the possible effect the pipelines may have on a current flowing along a sloping bottom.*

In Appendix D an expression for the maximum down-slope transport,  $Q_{\max}$ , for a cosine-shaped ridge is given. Simplifications may be made due to the small height of

the pipelines above the bottom and in this limit the shape of the obstacle becomes irrelevant. The upper limit for a possible down-slope transport is then given by

$$Q_{\max} = \frac{1}{2} \frac{g'}{f} H_R^2$$

With  $H_R=1.0$  m (the height of the pipelines) and  $g'=6 \times 10^{-2} \text{ ms}^{-2}$ , the maximum down-slope flow is around  $250 \text{ m}^3/\text{s}$ . If the total inflow is approximated to  $15\,000 \text{ m}^3/\text{s}$ , the down-slope flow must be less than 1.7 % of this value. This is a conservative estimate since the deep-water flow rate downstream of the Bornholm Strait will increase due to mixing and at the same time the value of  $g'$  will be reduced.

Considering the topography of the Bornholm Basin and that the mixing properties of a diverted flow will be the same as for the main inflow it is concluded that the effect of a possible down-slope steering of the inflow will be negligible.

Topographic steering is not relevant for the Gotland Basin since the pipelines do not cross the path of the inflowing water on any sloping bottom where this effect could play a role.

## 9 Creation and effects of pipeline dams

The establishment of pipelines may create closed depth contours and the area enclosed by these may be filled with denser water when the deepwater moves up and down along the bottom. Dams created by pipelines are not deeper than the height of the pipelines. If the denser water filling the dams can stay in the dams for sufficiently long time the oxygen in the dam may be exhausted by consumption and the phosphorus bound to metals at the surface of the sediments may be released to the dam water. The total area of possible pipeline dams in depth interval 40-80 m has been estimated to  $25 \text{ km}^2$  for the whole stretch of the pipeline (R. Bijker, 2009, pers. comm.). The estimate was made for an assumed pipeline height of 1.5 m which is conservative because the mean height will be 1.0 m. The estimated pool area is only about 0.06% of the bottom area in this depth interval why one may neglect the influence of pipeline dams on the phosphorus budget of the Baltic proper.

## 10 Effects on stratification and oxygen conditions in the Baltic Proper

The new deepwater flowing through the Arkona and Bornholm Basins supplies oxygen and salt to the deepwater of the Baltic Proper. It is therefore vital for the physical, biogeochemical and ecological states of the Baltic Proper. The properties of the new deepwater are subjected to quite large natural changes in these basins due to entrainment of residing less saline and oxygen rich water.

At present the turbulence created by the dense bottom current is due to bottom and interfacial friction. The total dissipation of the dense bottom current, i.e. the dissipation integrated from the entrance sills in Fehmarn Belt and Öresund to Stolpe Channel, is essentially determined by the potential energy of the dense water when passing the sills. The mixing of new deepwater might increase if the mixing efficiency of pipeline-generated turbulence is greater than that of turbulence generated by the present combination of bottom and interfacial friction.

It was found in Section 8.1 that if the Nord Stream pipelines rise 1.0 m above the sea bed they are capable to dissipate up to about 0.5 % of the total potential energy, depending on the speed of the dense bottom current in the crossing section. If the mixing efficiencies were equal there should in essence be no impact of the pipelines on the properties of new deepwater. We estimated that the mixing of the new deepwater might increase by 0-1.0%.

The effect of increased mixing by the pipelines on the inflow of new deepwater can be estimated as follows. The mean flow of water into the Baltic proper equals  $Q_{in}$  and it has the salinity  $S_{in}$  (c.f. *Figure 20*). These quantities can be estimated using conservation of salt and volume and knowing the freshwater supply  $Q_f$  and the salinity  $S_1$  of the water flowing out of the Baltic proper. With  $Q_f=15,000 \text{ m}^3\text{s}^{-1}$  and  $S_1=8.5$  psu one obtains  $Q_{in}=15,000 \text{ m}^3\text{s}^{-1}$  and  $S_{in}=17$  psu. Due to mixing with ambient water in the Arkona and Bornholm Basins, the flow of new deepwater increases by a factor  $E (>1)$  and the salinity decreases. The mean flow of new deepwater out of the Bornholm Basin equals

$$Q_2 = EQ_{in}$$

and its salinity is  $S_2$ . The relationship between  $E$  and  $S_2$  is obtained from the following equation for salt conservation

$$S_{in}Q_{in} + (E - 1)Q_{in}S_1 = S_2Q_2$$

If  $S_2=12$  psu one obtains  $E=2.43$  and  $Q_2=36450 \text{ m}^3\text{s}^{-1}$ . Due to extra mixing by the pipelines, entrainment of ambient water will increase  $x \cdot (E-1)Q_{in}$  where  $x$  is the increased mixing rate. A conservative estimate above gave that  $x$  is in the interval 0-0.010. This means that  $Q_2$  should increase by 0-215  $\text{m}^3\text{s}^{-1}$ , and  $S_2$  should decrease by at 0-0.02 psu.

The total negative buoyancy flux (by the new deepwater) into the Baltic proper is proportional to  $Q_2 \cdot (S_2 - S_1)$  and that quantity does not change with increased entrainment  $E$ . The depth of the halocline in the Baltic proper is adjusted so that the negative buoyancy flux is eroded into the surface layer by wintertime convection. Thus, the depth of the halocline, and thereby the volume of the deepwater, should not change with an increased  $E$ . This means that the flushing of the deepwater increases with  $E$ .

The oxygen transport, by new deepwater, increases with the volume flow provided the mixing occurs in areas where the ambient water is oxygenated, cf. last paragraph in Chapter 3. An increased transport of oxygen would tend to improve the oxygen conditions in, and below, the halocline in the Baltic Proper and thereby e.g. increase the deposition of phosphorus in the deepwater. This conclusion is supported by results reported by Gustafsson et al. (2008) who made numerical computations of effects of artificial halocline ventilation using two different state-of-the-art Baltic Sea models. Both models showed that increased mixing of halocline water (halocline ventilation) gives improved oxygen conditions in the Baltic proper. Considering much larger artificial mixing than that due to two pipelines discussed here, they concluded that because the decreased deepwater salinity, in the case considered by them, is within the range of natural variability it should not affect biodiversity.

The decrease in salinity due to extra mixing by the pipelines was shown above to be in the interval 0-0.02 psu which is very small compared to the range of natural variability (see Appendix A where it is shown that the standard deviation in salinity

in East Gotland Basin (stn BY 15) is about 0.5 psu in and below the halocline). One should therefore not expect that the flow of deepwater to northern parts of Baltic proper and to the Finnish Bight should be affected. This is also supported by Gustafsson et al. (2008) who did not report flow reductions to the northern regions although they considered much larger density reductions.

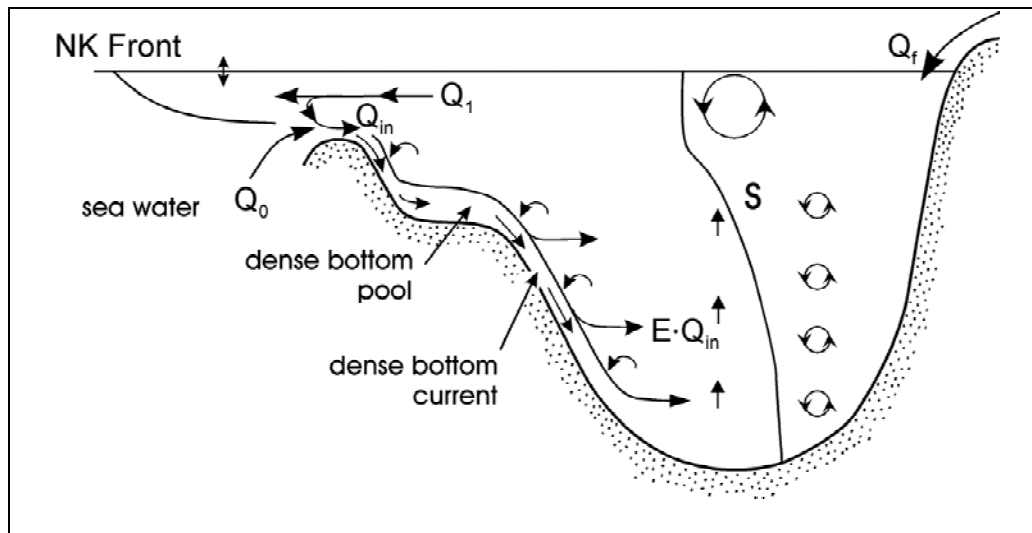


Figure 20. The inflowing dense water is a mixture between seawater from Skagerrak, volume flow  $Q_0$  and surface water coming from the Baltic. The volume flow of new deepwater entering the Baltic proper equals  $Q_{in}$ . Ambient water is entrained in the Baltic proper whereby the volume flow increases by the factor  $E$ .

## 11 Conclusions

In this report we estimate the impact of the planned Nord Stream pipelines on the salinity, volume flow and oxygen concentration of new deepwater in the Baltic Proper. The following findings were made:

- The mixing of the new deepwater might increase by 0-1.0%.
- The salinity of the new deepwater might decrease by 0-0.02 psu.
- The natural variability in and below the halocline in the East Gotland Basin is around 0.5 psu.
- Flows of volume, salt and oxygen might increase by 0-1.0%.
- If topographic steering takes place it can affect at most 1.7% of the inflow.
- The pipelines will have no hydraulic effect on the inflow.
- Dams (closed depth contours) created by the pipeline have no significant importance on the phosphorus dynamics.
- The pipelines will have no effect on, or possibly slightly counteract, eutrophication in the Baltic Proper.

From these findings one can conclude that the impact of the pipelines on the deep water in the Baltic Proper will be negligible.



## 12 References

- Alexandersson, H., 2006. Vindstatistik för Sverige 1961-2004. SMHI, Meteorologi Nr. 121.
- Arneborg, L., 2002. Mixing efficiencies in patchy turbulence. *Journal of Physical Oceanography*, 32(5), 1496-1506.
- Arneborg, L., Erlandsson, C.P., Liljebladh, B. and Stigebrandt, A., 2004. The rate of inflow and mixing during deepwater renewal in a sill fjord. *Limnology and Oceanography* 49, 768-777.
- Arntsen, Ø.A., 1996. Disturbances, lift and drag forces due to the translation of a horizontal circular cylinder in stratified water. *Experiments in Fluids*, 21, 387-400.
- Borenäs, K., and P. Lundberg, 1986. Rotating hydraulics of flow in a parabolic channel, *Journal of Fluid Mechanics* 167, pp. 309-326.
- Borenäs, K., R. Hietala, J. Laanearu, and P. Lundberg, 2007. Some estimates of the Baltic deep-water transport through the Stolpe trench. *Tellus A*, doi: 10.1111/j.1600-0870.2006.00221.x
- Burchard, H, Lass, H.U., Mohrholz, V., Umlauf, L., Sellchopp, J., Fiekas, V., Bolding, K., and Arneborg, L., 2005. Dynamics of medium-intensity dense water plumes in the Arkona Basin. *Ocean Dynamics* (Accepted)
- E. Darelus and A. Wåhlin, 2007. Downward flow of dense water leaning on a submarine ridge. *Deep Sea Research I*, Volume 56(7).
- Ellison, T.H., and Turner, J.S., 1959. Turbulent entrainment in stratified flows. *Journal of Fluid Mechanics* 6, pp. 423-448.
- Fischer, H., and W. Matthäus, 1996: The importance of the Drogden Sill in the sound for major Baltic inflows. *Journal of Marine Systems* 9, pp. 137-157.
- Gargett, A.E., and Holloway, G., 1984. Dissipation and diffusion by internal wave breaking. *J. Mar. Res.*, 42, 15-27.
- Grace, R.A., 1971. Submarine pipeline design against wave action. *Look Lab/Hawaii*, vol. 2, no 2, 3-7.
- Gustafsson, B.G., 2003. A time-dependent coupled-basin model of the Baltic Sea. Earth Sciences Centre, Göteborg University, Rep. C47, 61 pp. (ISSN 1400-383X)
- Gustafsson, B.G. and Andersson, H.C., 2001. Modeling the exchange of the Baltic Sea from the meridional atmospheric pressure difference across the North Sea. *Journal of Geophysical Research* 106, pp. 19731-19744.
- Gustafsson, B.G., Meier, H.E.M., Savchuk, O.P., Eilola, K., Axell, L., and Almroth, E., 2008: Simulation of some engineering measures aiming at reducing effects from eutrophication of the Baltic Sea. Univ. of Gothenburg, Dept. of Earth Science Centre, report no. C82, 59 pp.
- Hagen, E. and Feistel, R., 2004. Observations of low-frequency current fluctuations in deep water of the Eastern Gotland Basin/Baltic Sea. *Journal of Geophysical Research* 109, C03044, doi:10. 1029/2003JC002017.

Håkansson, B., Broman, B. and Dahlin, H., 1993. The flow of salt and water in the Sound during the Baltic major inflow event January 1993. Publ. C.M. 1993/C:57 (V). Int. Council for exploration of the Sea, Copenhagen.

Lass, H.U., Mohrholz, V. and Seifert, T., 2001. On the Dynamics of the Pomeranian Bight. *Continental Shelf Research*, 21, pp. 1237-1261.

Lass, H.U. and Mohrholz, V., 2003. On dynamics and mixing of inflowing salt-water in the Arkona Sea. *Journal of Geophysical Research* 108, 3042, doi:10.1029/2002JC001465

Liljebladh, B. and Stigebrandt, A. 1996. Observations of the deepwater flow into the Baltic Sea. *Journal of Geophysical Research* 101, pp. 8895-8912.

Liungman, O., Rydberg, L. and Göransson, C.G., 2001. Modeling and observations of deep water renewal and entrainment in a Swedish sill fjord. *Journal of Physical Oceanography* 31, pp. 3401-3420

MacDonald, D.G. and Geyer W.R., 2004. Turbulent energy production and entrainment at a highly stratified estuarine front. *Journal of Geophysical Research* 109, C05004, doi:10.1029/2003JC002094

Matthäus, W. and Franck, H., 1992: Characteristics of major Baltic inflows – a statistical analysis. *Continental Shelf Research* 12, pp. 1375-1400.

Matthäus, W. and Lass, H.U., 1994. The recent salt inflow into the Baltic Sea. *J. Phys. Oceanogr.*, 25, 280-286.

Omstedt, A. and Axell, L.B., 2003. Modeling the variations of salinity and temperature in the large gulfs of the Baltic Sea. *Continental Shelf Research* 23, pp. 265-294.

Omstedt, A. and Nohr, C., 2004. Calculating the water and heat balances of the Baltic Sea using ocean modelling and available meteorological, hydrological and ocean data. *Tellus* 56A, pp. 400-414.

Osborn, T.R., 1980. Estimates of the local rate of diffusion from dissipation measurements. *Journal of Physical Oceanography*, 10, 83-89.

Pedersen, B.F., 1980. A monograph on turbulent entrainment and friction in two-layer stratified flow. Series Paper No. 25, Inst. of Hydrodynamics and Hydraulic Engineering, Technical University of Denmark, Lyngby, 397 pp.

Petrén, O. and G. Walin, 1976. Some observations of the deep flow in the Bornholm strait during the period June 1973-december 1974. *Tellus*, 28, 74-87.

Piechura, J. and Beszczyńska-Möller, A. 2003. Inflow waters in the deep regions of the southern Baltic Sea – transport and transformations. *Oceanologia* 45, pp. 593-621.

Prastowo, T., R.W. Griffiths, G.O. Hughes, and A.M. Hogg., 2009: Effects of topography on the cumulative mixing efficiency in exchange flows. *J. Geophys. Res.*, vol 114, C08008, doi:10.1029/2008 JC005152.

Rydberg, L., 1976. Observations at the deep water flow through the Stolpe Channel during August 1976. Report No 15, Department of Oceanography, Göteborg University.

Rydberg, L., 1980. Rotating hydraulics in deep-water channel flow. *Tellus* 32 77-89.

Schimmels, S., 2007. Numerical Simulation of the Influence of Circular Cylinders on Mixing and Entrainment in Natural Density Currents. *Zur Erlangung des akademischen Grades Doktor der Ingenieurwissenschaften an der Fakultät für Bauingenieurwesen und Geodäsie der Gottfried Wilhelm Leibniz Universität Hannover vorgelegte Dissertation.*

Schinke, H. and W. Matthäus, 1998. On the causes of major Baltic inflows -- an analysis of long time series. *Continental Shelf Research* 18, pp. 67-97.

Simpson, J.H. and Rippeth, T., 1993. The Clyde Sea: A model of the seasonal cycle of stratification and mixing. *Estuarine Coastal and Shelf Science*, 37, 129-144.

Sivkov, V.V and N.I. Sviridov, 1994. The relation between erosional-accumulative forms of bottom relief and nearbottom currents in the Bornholm deep. *Oceanology*, Vol. 34, no.2.

St. Laurent, L. and Schmitt, R.W., 1999. The contribution of salt fingers to vertical mixing in the North Atlantic tracer release experiment. *Journal of Physical Oceanography*, 29, 1404-1424.

Stigebrandt, A., 1980: Barotropic and baroclinic response of a semi-enclosed basin to barotropic forcing from the sea. In *Fjord Oceanography* (H.J. Freeland, D.M. Farmer and C.D. Levings, eds.). Plenum, New York, pp. 151-164.

Stigebrandt, A., 1983: A model for the exchange of water and salt between the Baltic and the Skagerrak. *J. Phys. Oceanogr.*, 13, 411-427.

Stigebrandt, A., 1985. A model for the seasonal pycnocline in rotating systems with application to the Baltic proper. *Journal of Physical Oceanography* 15, pp. 1392-1404.

Stigebrandt, A., 1987a. A model for the vertical circulation of the Baltic deep water. *Journal of Physical Oceanography* 17, 1772-1785.

Stigebrandt, A., 1987b: Computations of the flow of dense water into the Baltic Sea from hydrographical measurements in the Arkona Basin. *Tellus* 39A, pp. 170-177.

Stigebrandt, A., 2001: Physical Oceanography of the Baltic Sea. Chapter 2 (pp. 19-74) in *A systems Analysis of the Baltic Sea* (F. Wulff, L. Rahm and P.Larsson, eds.), Springer Verlag.

Stigebrandt, A. and B.G. Gustafsson, 2007. Improvement of Baltic proper water quality using large-scale ecological engineering. *AMBIO*, 36, 280-286.

Stigebrandt, A. Johnsson, M. and Wüest, J., 2006: Mixing efficiency of turbulence in dense gravity-forced bottom currents. In Johnsson, M., 2006: Studies in coastal seas of small scale mixing processes related to topography. Göteborg University, Oceanography/Earth Sciences Centre, Publ. A106 (Licentiate thesis).

Tinis, S.W. and Pond, S., 2001. Tidal energy dissipation at the sill of Sechart Inlet, British Columbia. *Journal of Physical Oceanography*, 31, 3365-3373.

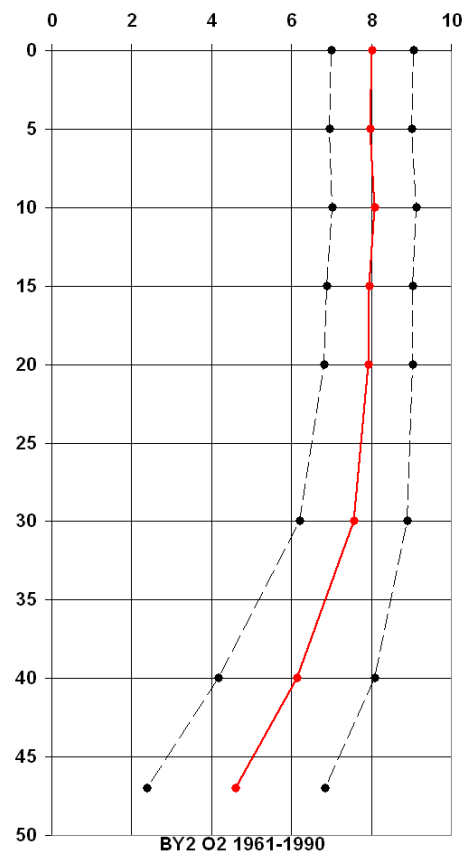
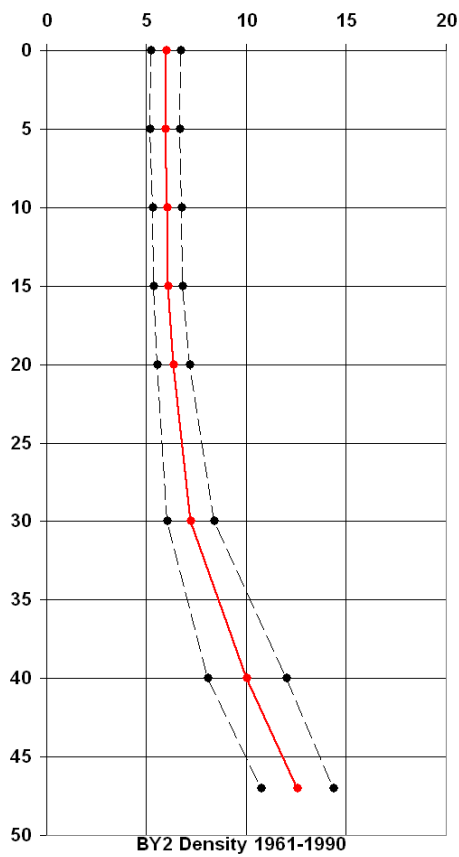
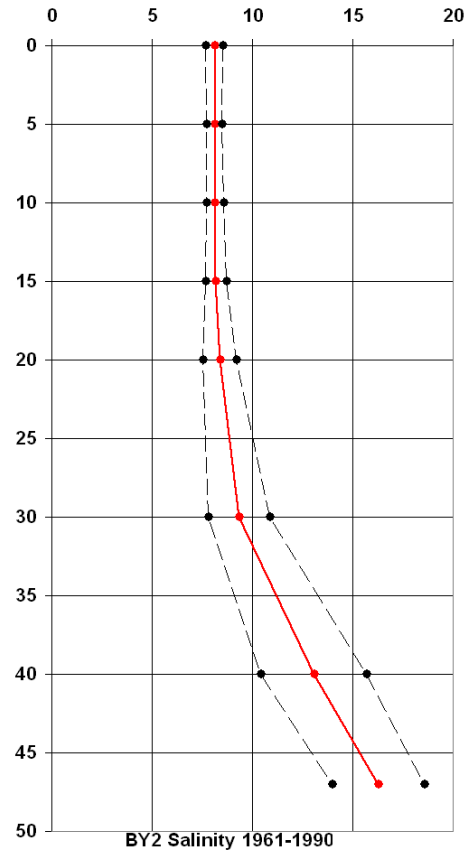
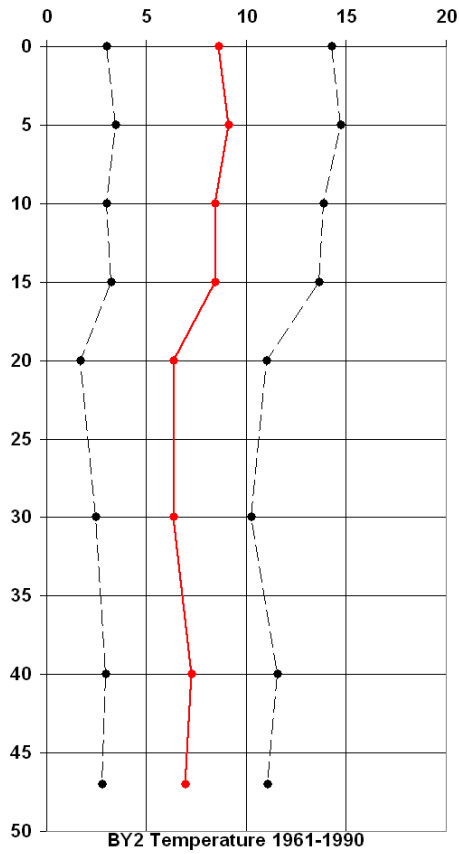
Whitehead, J., Leetma, A. and Knox, R. 1974. Rotating hydraulics of strait and sill flows. *Geophys. Fluid Dyn.* 6 101-125

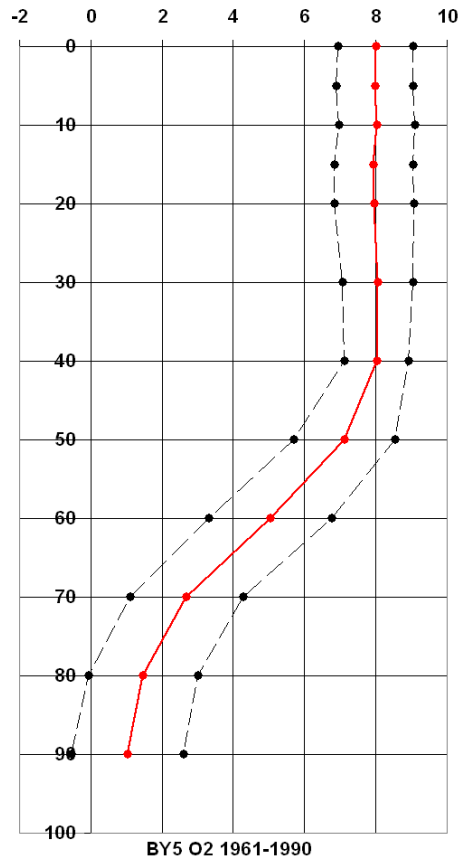
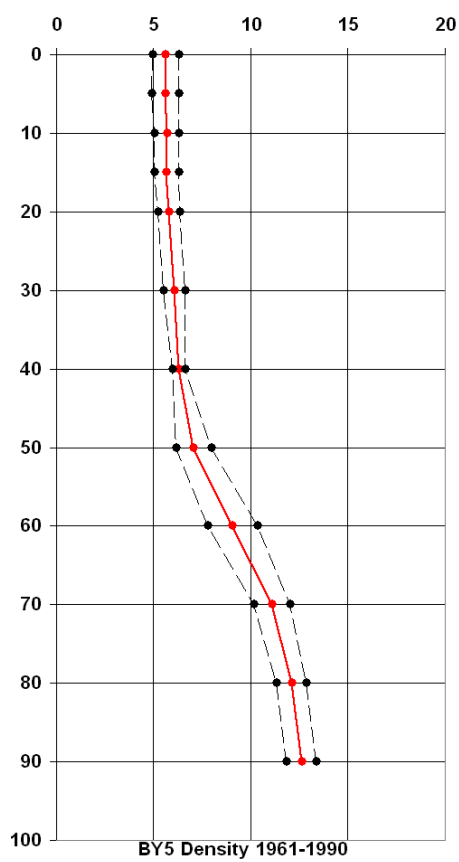
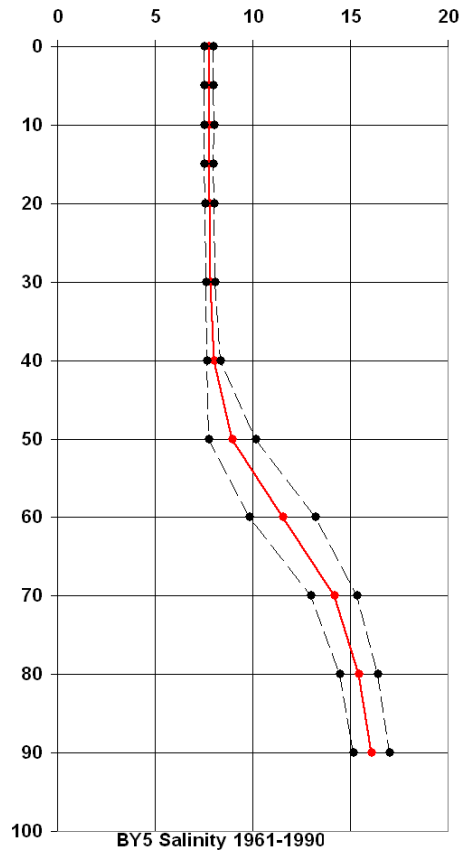
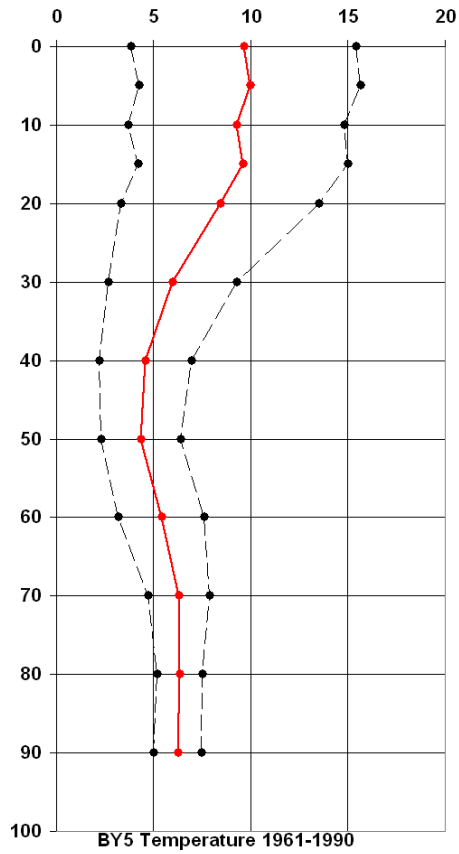
## 13 Appendices

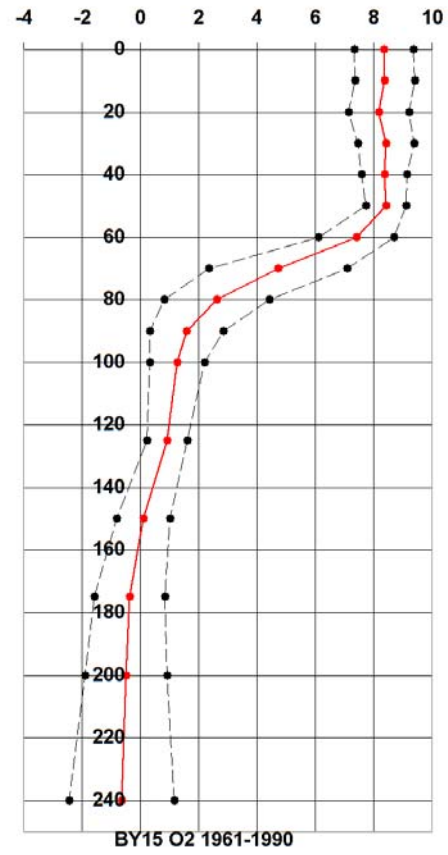
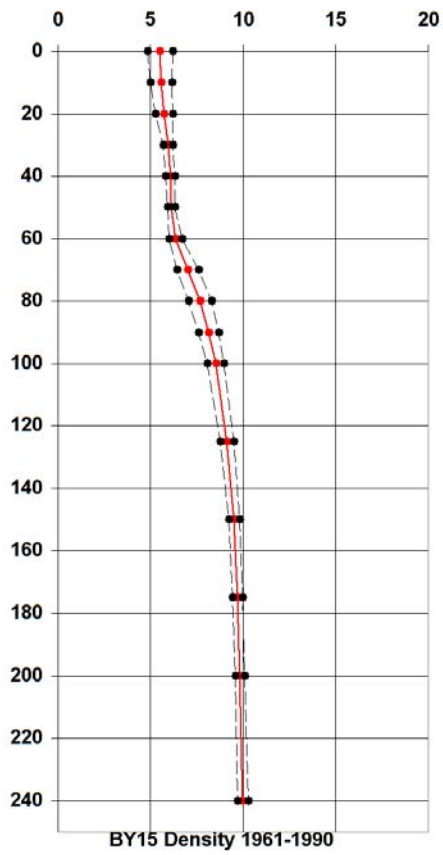
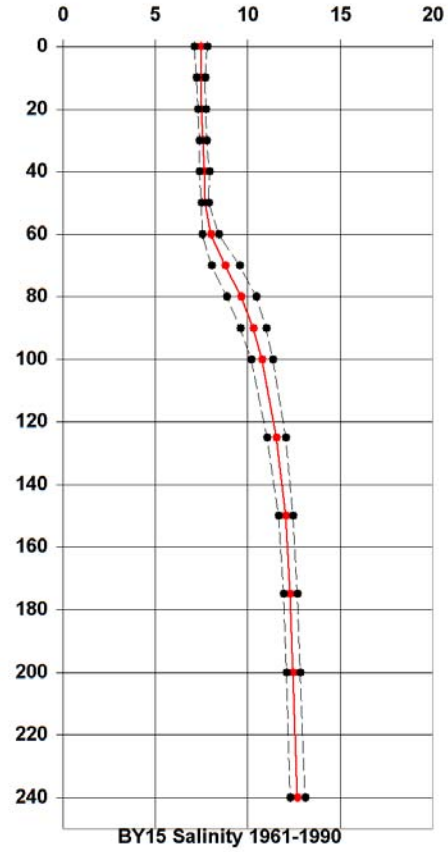
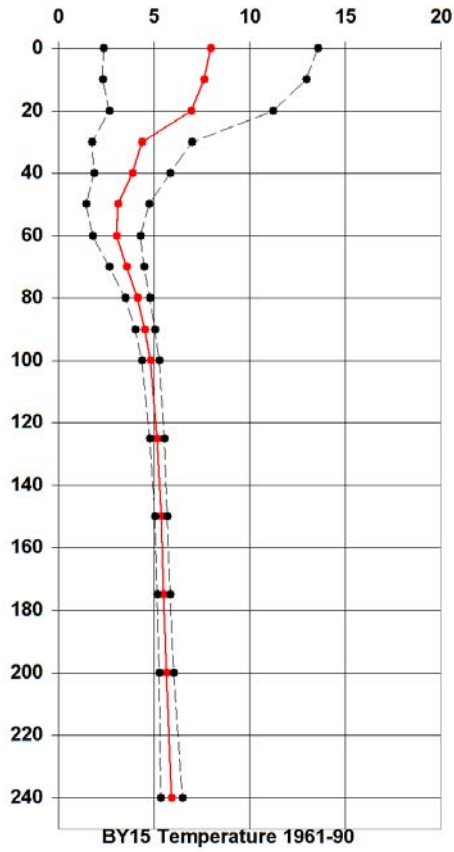
### Appendix A

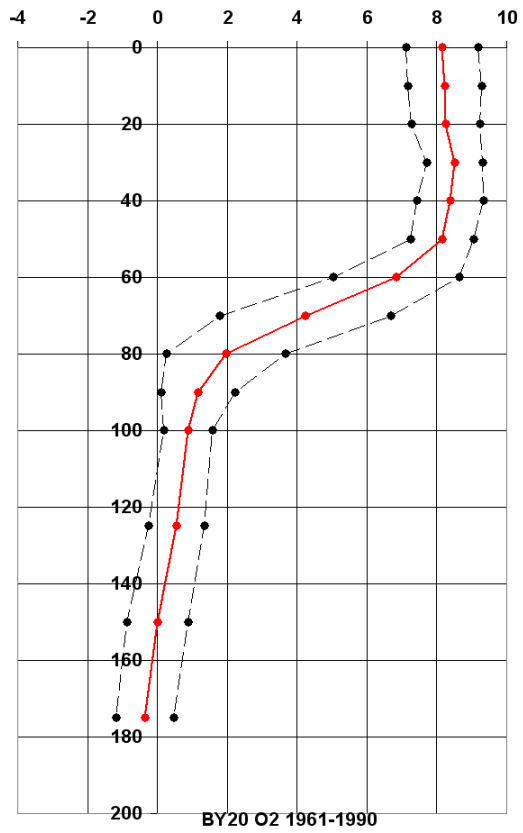
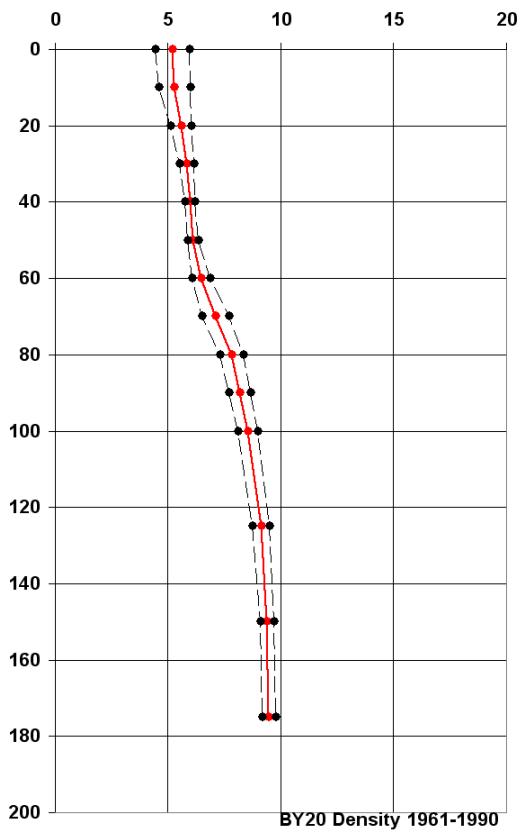
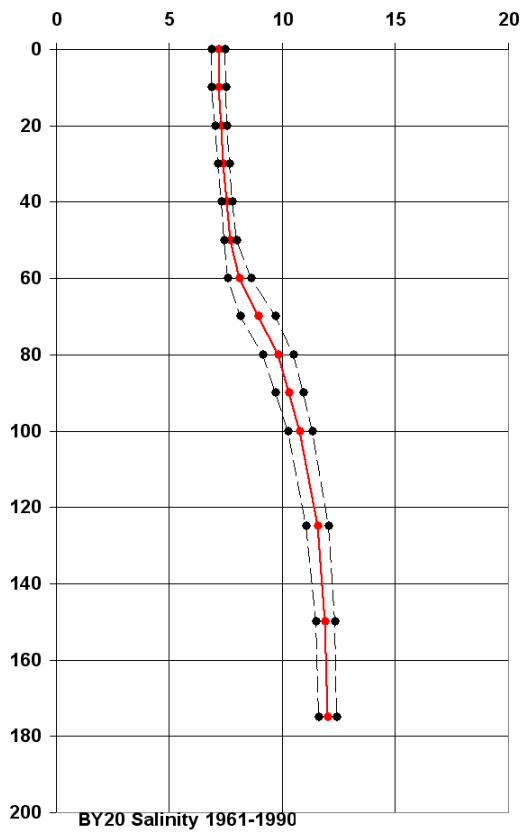
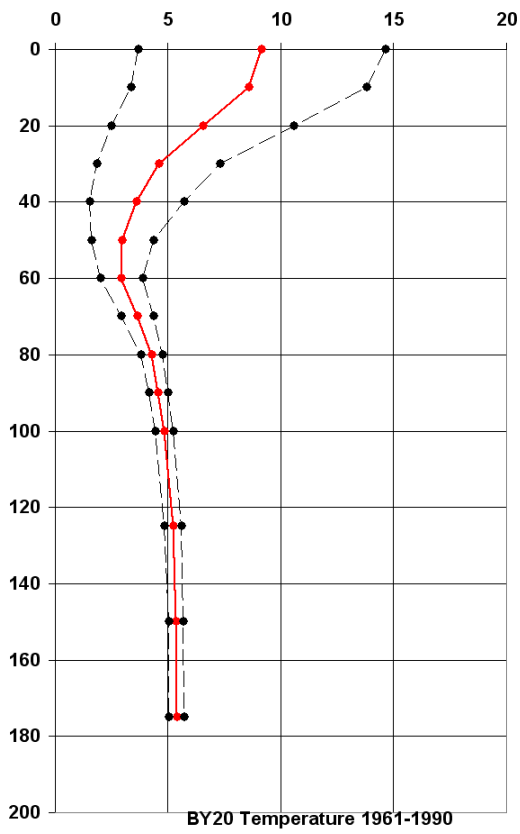
Climatological averages (red) and standard deviations (black) for vertical profiles of temperature ( $^{\circ}\text{C}$ ), salinity, density ( $\sigma_t$ ,  $\text{kg/m}^3$ ) and oxygen ( $\text{ml/l}$ ) at stations BY2, BY5, BY15 and BY20, based on observations gathered for the period 1961-1990. For positions see map below.













## Appendix B

Jan	Feb	Mar	Apr	May	Jun	Jul	Aug	Sep	Oct	Nov	Dec	Year
7.8	6.9	7.0	6.2	5.9	5.9	6.2	6.0	7.0	7.6	8.4	8.1	6.9

Mean values of the wind speed (m/s) at Falsterbo for the period 1961-1990.

Jan	Feb	Mar	Apr	May	Jun	Jul	Aug	Sep	Oct	Nov	Dec	Year
6.9	6.8	6.2	5.4	5.2	5.6	4.9	5.3	5.9	6.6	6.8	6.9	6.0

Mean values of the wind speed (m/s) at Falsterbo for the period 1991-2004.

N	NO	O	SO	S	SV	V	NV	Calm
7.4	6.3	13.9	10.9	12.8	15.8	20.7	10.6	1.5

Frequency of the wind direction (%) at Falsterbo for the period 1961-2004.



From Alexandersson (2006).

## Appendix C

### 1. Dynamics of a frictional dense bottom current

We consider new deepwater flowing over a sill into a basin where the deepwater forms an inclined gravity-forced plume that entrains ambient water. The plume eventually debouches into a pool of deepwater. It is assumed that the dense plume flows in a channel of width  $W$ . The channel has the longitudinal slope  $s$  relative the horizontal plane. If  $d$  is the vertical thickness and  $U$  the speed of the plume, the volume flow  $Q$  of the plume is given by

$$Q = UWd \quad (C1)$$

The (quasi) steady-state flow is governed by a balance between the longitudinal (down-slope) pressure gradient force and frictional forces, the latter are quadratic and described by the combined (bottom and interfacial) drag coefficient  $C_D$ . Thus

$$U = \sqrt{\frac{g' ds}{C_D}} \quad (C2)$$

Here  $g' = g\Delta\rho/\rho_0$  is the reduced gravity with  $\Delta\rho = \rho_1 - \rho_2$  and  $\rho_0$  is a reference density.

The transport per unit width is defined by  $q = Ud = Q/W$  and the buoyancy flux is  $b = g'q$ . Stigebrandt (1987a) derived the following expressions for the speed and thickness of the plume

$$U = \left(\frac{s}{C_D}\right)^{\frac{1}{3}} b^{\frac{1}{3}} \quad (C3)$$

$$d = \left(\frac{s}{C_D}\right)^{-\frac{1}{3}} \left(\frac{q^2}{g'}\right)^{\frac{1}{3}} \quad (C4)$$

Since the fluids are miscible, turbulence generated by the plume may cause entrainment of less dense fluid into the bottom current whereby the volume flow increases and the density decreases. The entrainment velocity  $w$  is given by the following energy-based Kato-Phillips type of expression used for two-layer systems, c.f. Turner (1973)

$$w = 2m_0 \frac{u_*^3}{g'd} \quad (C5)$$

Here  $m_0$  is a constant (e.g. Stigebrandt, 1985). The friction velocity  $u_*$  is defined by

$$u_*^2 = C_D U^2 \quad (C6)$$

Stigebrandt et al. (2006) used the model above to estimate the effective value of  $Rf$  by deriving the ratio between the buoyancy flux by the entraining flow and the power supplied to turbulence by bottom and interfacial drag. They obtained

$$Rf = m_0 C_D^{1/2} \quad (C7)$$

Using  $m_0 = 0.6$  as determined from a seasonal pycnocline model applied to the Baltic Sea (Stigebrandt, 1985), and a value of the combined  $C_D$  in the range 0.003 – 0.005 gives  $Rf$  in the range 0.033 – 0.042. They also analyzed results of laboratory experiments on entrainment by dense bottom currents conducted by Ellison and Turner (1959), displayed in Fig. 6.10 in Turner (1973), and found that  $Rf$  equals about 0.03 for rather steep slopes ( $s > 0.17$ ). Results from hydrographic measurements in the dense bottom current in Denmark Strait presented by Pedersen (1980), also support a value of  $Rf$  in the range 0.03 to 0.04. One may thus conclude that the efficiency of turbulence generated by combined bottom and interfacial drag in dense bottom currents equals approximately 0.04. For other types of stratified flows  $Rf$  might have different values, see below.

The total entrainment of ambient water, from the intrusion of new deepwater at the entrance sills until it reaches the top of the dense water pool at depth  $h_1$ , equals

$$Q_e = W^{2/3} 2Rf \left( \frac{s}{C_D} \right)^{1/3} B^{1/3} h_1 \quad (C8)$$

Here  $B=bW$  is the total buoyancy flux by the dense bottom current. Eq. (C8) shows that the entrainment will vary with the width (height) of the current. Thus, even if the flux Richardson number is constant and known, the resulting mixing varies with the geometry of the current. Eq. (C8) shows that a wide (and accordingly thin) current entrains more than a narrow current.

In the present case it is believed that the dense bottom current will not change its width due to the crossing of the pipelines. However, the pipelines will induce so-called form drag on the current which in turn creates turbulence that might have an other efficiency with respect to diapycnal mixing than ordinary bottom and interfacial mixing.

The total dissipation by the dense bottom current between the entrance sills and Stolpe Channel, where the outlet of dense water from the Bornholm Basin occurs, can be estimated as

$$D_0 = LWUS \quad (C9)$$

where  $L$  is the length and  $W$  the typical width and  $U$  the typical velocity of the dense bottom current.  $S$  is the bottom stress computed from  $S = \rho_0 C_D U^2$  and  $C_D$  is the coefficient for combined bottom and interfacial drag and  $\rho_0$  is a standard density. The dissipation caused by the crossing pipeline of height  $h$  equals

$$D_p = WUh\rho_0 C U^2 \quad (C10)$$

where  $C$  is the coefficient for form-drag caused by a pipeline resting on the bottom. Typical values of the drag coefficients are  $C_D = 0.003$  and  $C = 1.5$ , see below, and we have assumed that the current in the crossing section has the typical speed and width. This means that one pipeline of height  $h = 1.0$  m exerts a drag equivalent to the frictional drag along a stretch of about 500 m.

The dissipation of energy by the dense water from the entrance sills to the Stolpe Channel can also be estimated from the following equation

$$D_0 = \rho_0 Q g' h_1 \quad (C11)$$

Here  $Q$  is the flow and  $g'$  the (negative) buoyancy of new deepwater and  $h_1$  is the depth below the sea surface of the deepwater pool in the Bornholm Basin. Combining Eqs. (C10) and (C11) one might estimate typical values of  $U$  and  $W$  in the Arkona and Bornholm Basins. This is done in Chapter 8.1 of the present report.

## 2. Dissipation and drag caused by a pipeline

The dissipation caused by a pipeline is proportional to the height  $h$  of the pipeline and the cubed speed of the crossing current, c.f. Equation (C10). The coefficient of proportionality, the form drag, in homogeneous water is known from many earlier investigations. For a flow past a circular cylinder the drag coefficient,  $C$ , is a function of the Reynolds number,  $Re$ , the ratio of the inertia to the viscous force. For  $Re$  less than about 200,000 the drag coefficient is about 1.2 and it drops to less than 0.5 for higher  $Re$ , see e.g. Schimmels (2007). In the present application  $Re$  typically equals  $3 \cdot 10^5$ . The secondary motion induced by the drag in homogeneous water takes the form of eddies that are shed from the pipe.

Based on wave tank experiments Grace (1971) recommended a value of  $C=2$  for a pipeline on the seafloor with no spacing between the pipe and the bottom. This value was suggested for estimating the forces *acting on the pipeline*, and may hence be considered to be conservative. Grace also carried out experiments outside Hawaii with a pipe placed on the bottom in the wave zone. The pipe had a diameter of 0.3 m and the water depth was 5m. The measured drag coefficient had a mean of 1.2 with the minimum and maximum values being 0.5 and 1.4, respectively.

In vertically stratified water, the drag may vary with the densimetric Froude number,  $F = U/c_i$ , where  $U$  is the speed of the crossing current and  $c_i$  is the phase speed of the lowest mode of internal waves. Arntsen (1996) made laboratory studies of the drag on a moving horizontal cylinder submerged in a stratified fluid with two homogeneous layers of different density separated by a thin pycnocline. The baroclinic drag takes the form of internal waves behind the cylinder and is similar to so-called dead-water affecting slow ships in stratified waters that was described and analyzed by (Ekman, 1904). In the experiments,  $1000 < Re < 10,000$  which is an order of magnitude less than in the Bornholm Basin situation. Arntsen (1996) found that the drag coefficient under stratified conditions,  $C$ , may have values up to about 2 for small  $F$ . For Froude number greater than about 0.6 the drag was found to be even slightly less than for non-stratified conditions. These results were valid for cases when the horizontal cylinder was above or below the pycnocline. When the cylinder was at the level of the pycnocline the stratification actually decreased the drag as compared to non-stratified conditions.

How can these results be used in the present investigation? One difference for the stratified case is that the pipelines are lying on the bottom. However, the baroclinic response of the flow, mainly for  $F < 0.6$ , should take the form of stationary internal waves, i.e. waves in the stratification bound to, and on the lee-side of, the pipelines (lee-waves). Due to mixing induced by bottom friction, the thickness of the homogeneous bottom layer should increase with the speed of the bottom layer and a crossing pipeline should induce a combination of barotropic and baroclinic drag. The

baroclinic contribution to the drag should decrease with increasing thickness of the homogeneous bottom layer.

For our computations of the contribution of the pipelines to total dissipation we have implicitly used the speed 0.3 m/s for the bottom current. By determining the stratification in the Bornholm Basin from observations (Chapter, 4.4) under conditions with dense bottom currents, shown by a homogeneous bottom layer in CTD-profiles, we can also estimate the maximal speed of internal waves and thereby we can assess the value of  $F$  in situations with dense bottom currents. We are thereafter in the position to discuss appropriate values of  $C$  for our estimates.

For 46 (out of 240) profiles it was possible to judge whether there was a homogeneous bottom layer present or if the layer below the halocline was stratified all the way to the bottom. A mixed bottom layer was found in 27 profiles for which the velocity of the lowest internal wave mode was calculated. It was found that the mean value of  $c_i$  was 0.55 m/s with a standard deviation of 0.18 m/s. The corresponding mean value for  $F$  was 0.54. In these cases stratification should influence  $C$  although the pipelines are embedded in a homogeneous (mixed) bottom layer.  $C=1.5$  seems to be a reasonable mean value of the form drag for these cases. A similar calculation was also carried out for the 19 cases of stratified bottom layer giving  $c_i=(0.4 \pm 0.14)$  m/s with the corresponding mean value of 0.75 for  $F$ . For such high values of  $F$  stratification should have small importance according to the experiments by Artsen (1996) and  $C$  should be less than 1.5. However, it is possible that  $U=0.3$  m/s is too high for these cases lacking a mixed layer, which would motivate a higher value of  $C$ . On the other hand, only a relatively small share of the total transport should be performed by these cases why they should be given only a small weight in determining  $C$ . All in all we conclude that using  $C=1.5$  would be conservative.

### 3. Mixing efficiency

There are two different definitions of mixing efficiency. The “process” definition focuses typically on one type of process, ideally localized in an infinitely small volume. The “system” or “bulk” or “overall” or “cumulative” definition aims at macroscopically large volumes of a natural volume water body. Determining “system” mixing efficiency might be difficult because one has to establish both the power supply to the turbulence and the resulting buoyancy fluxes. Reliable energy budgets have been established for fjord basins, where the main power input to turbulence comes via internal tides and the buoyancy fluxes resulting from vertical mixing may be estimated from repeated measurements of the (changing) vertical stratification in periods when there is no advective water exchange. Numerous estimates for basin waters of fjords give (system)  $R_f$ -values in the range 0.05-0.08 as shown by Stigebrandt & Aure (1989). This is supported by many authors, e.g. Simpson & Rippeth (1993) and Tinis & Pond (2001). For dense bottom currents Stigebrandt et al. (2006) estimated that the system  $R_f$  equals 0.04 for natural flows and  $R_f=0.03$  for published laboratory flows.

Values of (process)  $R_f$  in the range 0.15-0.20, in essence based on laboratory experiments with rather differing results, have been widely used in oceanography, e.g. Osborn (1980), Gargett and Holloway (1984) and St Laurent and Schmitt (1999).

However, Arneborg (2002) has shown that numbers for process  $R_f$  estimated from laboratory experiments include both the work done against the buoyancy forces on the system level and short-lived potential energy in turbulent patches. The latter dissipates when patches collapse. Arneborg (2002) estimated that the system  $R_f$  should be slightly higher than half of the value of the process  $R_f$ . Accepting process  $R_f=0.20$  he finds that system  $R_f$  equals 0.11.

The systems or cumulative mixing efficiency of buoyancy-driven, hydraulically controlled laboratory flows was investigated by Prastowo et al. (2009). The overall amount of turbulent mixing was determined from measurements of vertical density profiles after the exchange. The systems mixing efficiency varied between 0.08 and 0.11 depending on the topography of the constriction.

In vertically stratified water, drag due to horizontal pipelines resting on bottom and perpendicular to the current direction might vary with the densimetric Froude number  $F=U/c_i$ , where  $U$  is the current speed and  $c_i$  the phase speed of the lowest mode of internal waves as discussed in Chapter C2 above. For  $F<1$  internal lee-waves may be generated. However, due to bottom friction there will be a several meter thick homogeneous layer nearest to the bottom (*c.f. Figure 9*) reducing the interaction between a 1.0 m high pipeline and the stratified water above the homogeneous bottom layer. It is therefore likely that the drag due to the pipelines mainly takes the form of eddies in the well-mixed bottom layer. This suggests that the system mixing efficiency of turbulence caused by the pipelines is similar to the system mixing efficiency in dense bottom currents, thus with  $R_f \approx 0.04$ . We have not found any published values of mixing efficiency of turbulence generated by neither horizontal pipes nor vertical cylinders in stratified flows. Computations in this report are done using system  $R_f=0.04$  and system  $R_{f_{\text{pipe}}}=0.12$ . The latter is higher than the highest published estimate of system  $R_f$  and should give a conservative upper limit of mixing effects of the pipelines on the system level, see the overview in Table C1.

Table C1. Overview of published  $R_f$ -values. S and P denotes the type of definition where S=System, P=process.

Rf value	Comments	References
0.05-0.08 S	Internal tides in fjord basins (numerous estimates)	Stigebrandt & Aure (1989), Simpson & Rippeth (1993), Tinis & Pond (2001)
0.04 S	Bottom gravity currents	Stigebrandt et al (2006)
0.11 S	Turbulent patches after gravitational collapse	Arneborg (2002)
0.08-0.11 S	Laboratory experiments with exchange flows	Prastowo et al. (2009)
0.15-0.20 P	Estimates for shear-induced turbulence in essence based on laboratory estimates	Osborn (1980), Gargett and Holloway (1984), St. Laurent and Schmitt (1999)

## Appendix D

### Topographically steered flows

According to Darelus and Wåhlin (2007) the maximum down-slope transport,  $Q_{\max}$ , for a cosine-shaped ridge is given by

$$Q_{\max} = \frac{g'}{f} H_R^2 \frac{\pi^2}{4} \left[ \frac{\pi^2(1 + e^{-\gamma})}{(\pi^2 + \gamma^2)^2} + \frac{\gamma}{2(\pi^2 + \gamma^2)} \right] \quad (\text{D1}).$$

Here  $g'$  is the reduced gravity,  $f$  the Coriolis parameter and  $H_R$  the height of the ridge (pipeline). The nondimensional quantity  $\gamma$  is defined as

$$\gamma = \frac{\alpha W_R}{\delta}$$

where  $\alpha$  is the slope parameter,  $W_R$  the width of the ridge (pipeline) and  $\delta$  the Ekman layer thickness. The Ekman layer may be approximated by

$$\delta = \frac{C_D U_\alpha}{f}$$

where  $C_D$  is the drag coefficient and  $U_\alpha$  the geostrophic velocity along the slope given by

$$U_\alpha = \frac{g' \alpha}{f}.$$

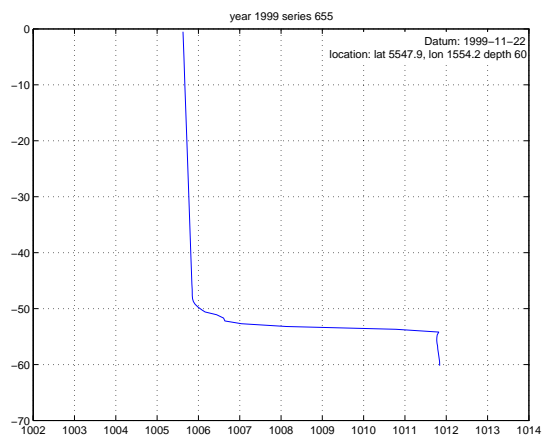
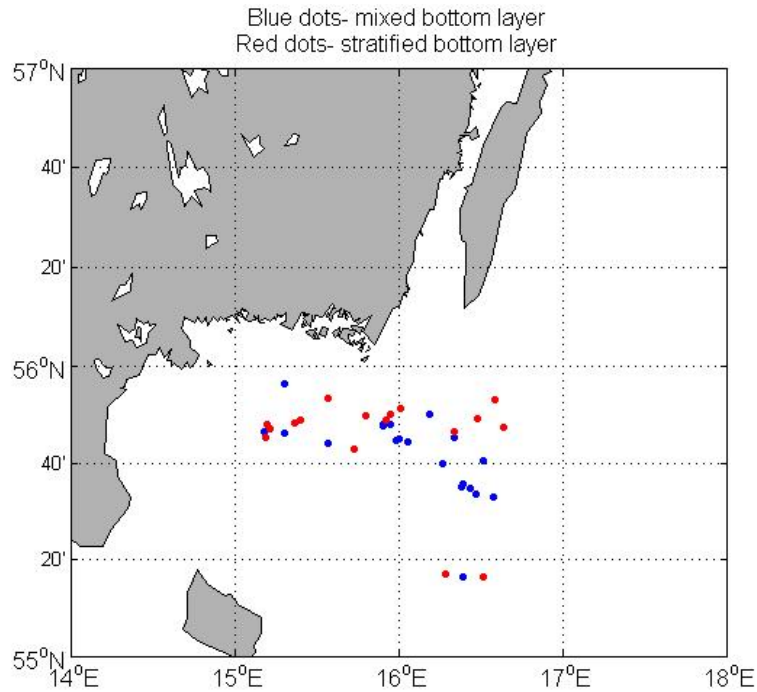
Inserting the following values:  $g'=6 \times 10^{-2} \text{ m/s}^2$ ,  $f=1.2 \times 10^{-4} \text{ s}^{-1}$ ,  $\alpha=1.2 \times 10^{-3}$ ,  $C_D=3 \times 10^{-3}$  and  $W_R=3 \text{ m}$ , yields  $\gamma=2.4 \times 10^{-4}$ . Since the value of  $\gamma$  is very small the maximum down-slope transport, in the limit  $\gamma \rightarrow 0$ , becomes

$$\lim_{\gamma \rightarrow 0} Q_{\max} = \frac{1}{2} \frac{g'}{f} H_R^2 \quad (\text{D2}).$$

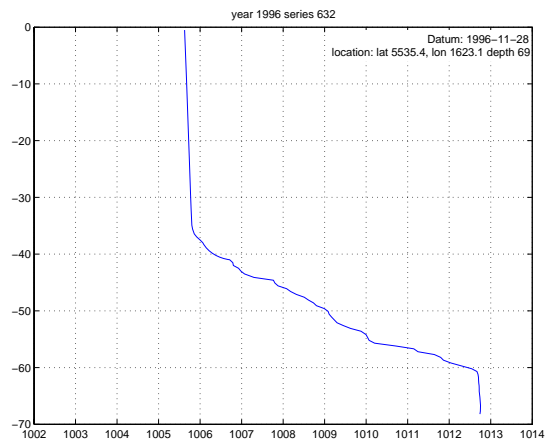
It should be mentioned that eq. (D2) holds for a variety of different shapes of the ridge in the limit  $\gamma \rightarrow 0$ .

## Appendix E

The positions of the 46 profiles discussed in Section 4.4 and Appendix C, together with some examples of density profiles.

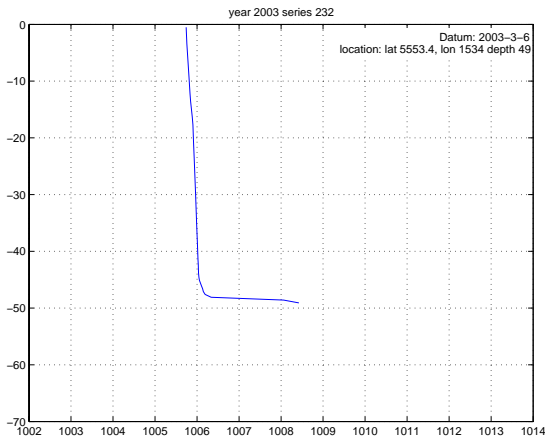


*Homogeneous bottom layer, thin pycnocline*

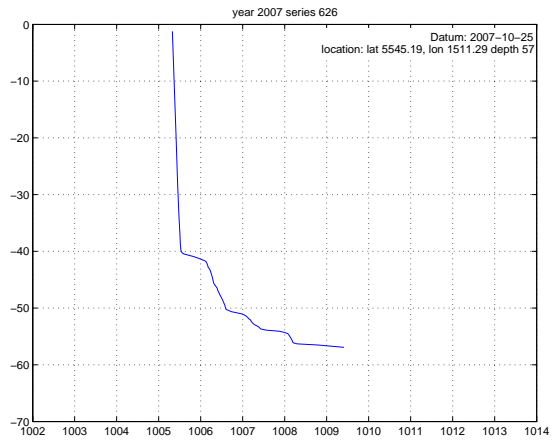


*Homogeneous bottom layer, thick pycnocline*





*Stratified bottom layer, thin pycnocline*



*Stratified bottom layer, thick pycnocline*





Swedish Meteorological and Hydrological Institute  
SE 601 76 NORRKÖPING  
Phone 011-495 80 00 Fax 011-495 80 01